Bio-Design and Manufacturing (2023) 6:563–585
https://doi.org/10.1007/s42242-023-00241-7

REVIEW

Recent advances in lung-on-a-chip technology for modeling respiratory disease

Jorge A. Tavares-Negrete[2,4] · Prativa Das[1,4] · Sahar Najafikhoshnoo[1,4] · Steven Zanganeh[6] · Rahim Esfandyarpour[1,2,3,4,5]

Received: 10 October 2022 / Accepted: 7 March 2023 / Published online: 13 June 2023

Abstract

Tissue engineering approaches, including those to functional lung tissues, are finely honed by the inclusion of upgraded devices that mimic biophysical and biochemical features in vivo. Perfusion culture is one of these essential biophysical characteristics enabled by the introduction of microfluidic devices in recent years. This review links the importance of dynamic culture for in vitro maintenance of functional lung cells to the modeling of respiratory disease. We identify and discuss different parameters for fabricating the requisite microfluidic models for lung cells, as well as their application in modeling lung diseases caused by external factors such as smoking and pollution. The possibility of creating a multi-organ-on-a-chip to establish a more physiologically relevant model is highlighted. Overall, the focus is on different prospects for the in vitro modeling approach and for lungs-on-a-chip for developing advanced, reliable technology to analyze the pathophysiology of respiratory diseases and screen potential treatments.

Jorge A. Tavares-Negrete and Prativa Das have contributed equally to this work.

✉ Rahim Esfandyarpour
rahimes@uci.edu

1 Department of Electrical Engineering, University of California, Irvine, CA 92697, USA

2 Department of Biomedical Engineering, University of California, Irvine, CA 92697, USA

3 Henry Samueli School of Engineering, University of California, Irvine, CA 92697, USA

4 Laboratory for Integrated Nano Bio Electronics Innovation, Henry Samueli School of Engineering, University of California, Irvine, CA 92697, USA

5 Department of Mechanical and Aerospace Engineering, University of California, Irvine, CA 92697, USA

6 Department of Bioengineering, University of Massachusetts Dartmouth, Dartmouth, MA, USA

Graphic abstract

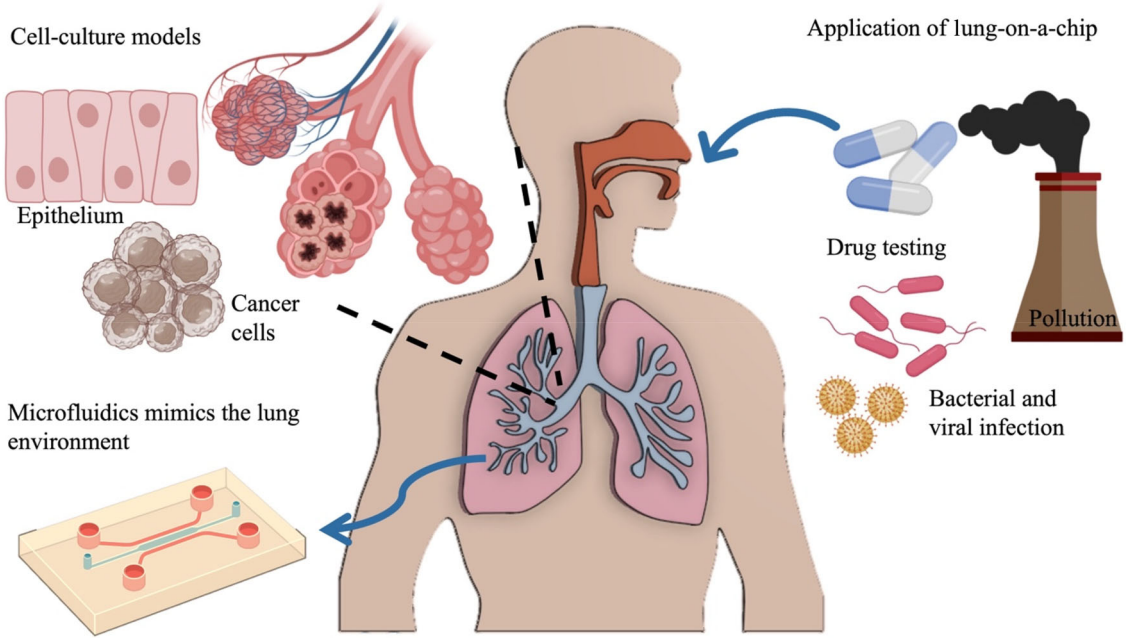

Keywords Lung-on-a-chip · In vitro modeling · Lung pathophysiology · Respiratory diseases · 3D culture model

Introduction

The prevalence of respiratory diseases results in about 4 million deaths worldwide every year and thus represents a major concern and an increasing healthcare burden on society [1]. As the foundational organ of the respiratory system, lungs are primarily responsible for facilitating gas exchange between the bloodstream and the environment. The primary bronchi, formed from the bifurcated trachea, are subdivided into the lobes, segmental bronchi, bronchioles, terminal bronchioles, and ultimately over 300 million alveoli [2]. Different lung diseases, e.g., chronic obstructive pulmonary disease (COPD), idiopathic pulmonary fibrosis (IPF), acute respiratory distress syndrome (ARDS), infectious diseases such as tuberculosis and pneumonia, and lung cancer, are identified as the prime cause of mortality in all countries [3, 4]. In recent years, the massive outbreak of SARS-CoV-2 also reportedly affected lung pathophysiology due to an inflammatory response induced by cytokine storm. This made it even more vital to develop a representative human lung model for disease analysis and preclinical validation of effective treatments [5, 6]. Researchers aimed at finding potential therapeutic approaches based on in vivo animal models have not been sufficient to establish reliable cures for human lung disease, due to the proven differences in pathophysiology, as well as genotypic variability [7]. Again, with increasing ethical concerns about using animals for research purposes, development of a representative in vitro model has become necessary for basic and preclinical research. The most common approach so far is two-dimensional (2D) monolayer culture of lung cells, which has failed to accurately represent the functional properties of the three-dimensional (3D) human tissue [8, 9]. Moreover, conventional 2D culture models [10] are unable to represent structural cues such as surface stiffness or mechanical cues such as shear stress and strain, which leads to significant alteration of cell morphology, physiological function, gene expression, kinetics of cell division, and type and quantity of cytokine secretion when compared to in vivo counterpart processes [11–13]. Relatively recently, microfabricated [14–18] microfluidic devices [17, 19–24] began to draw considerable attention for creating physiologically relevant gradient flow of media and other essential growth elements in in vitro mammalian cell cultures; they appear to offer an alternative to static culture models for achieving an organ-level dynamic microenvironment. Lung-on-a-chip devices obtained by combining modern tissue engineering with microfabrication techniques provide a new, effective, and reliable in vitro platform for screening potential drugs and efficiently modeling respiratory diseases (Fig. 1) [11]. These in vitro models can also allow the inclusion of human lung cells for analysis of metabolic, genetic, and biochemical activity, while providing

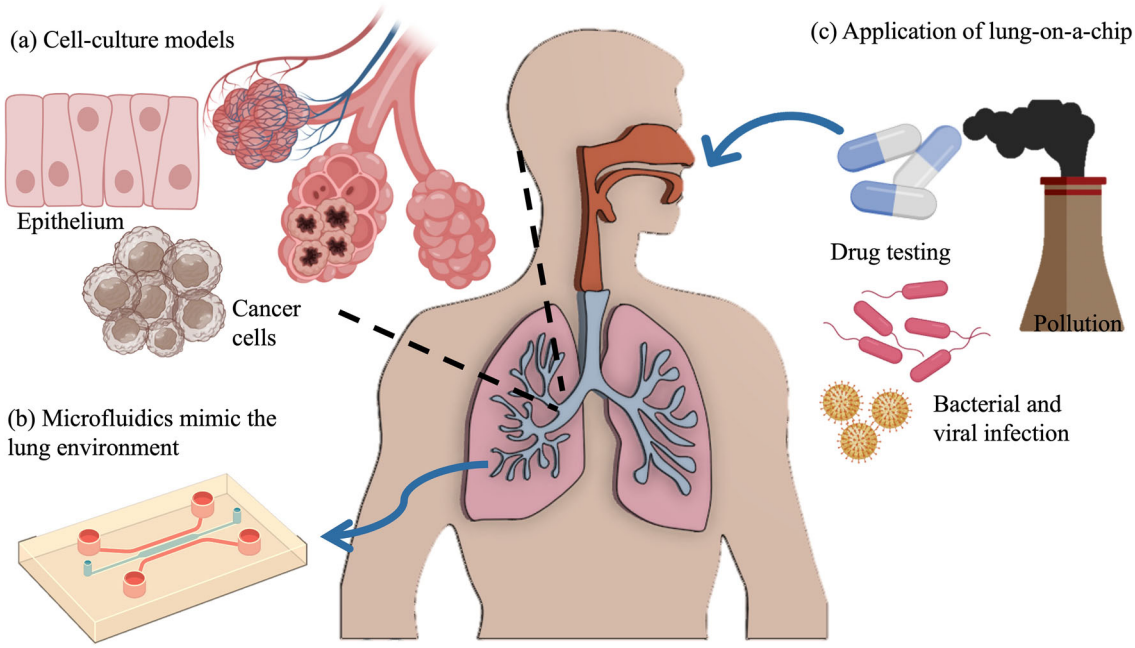

Fig. 1 Recapitulation of lung physiology using lung-on-a-chip systems. **a** The evolution of cell culture methods. **b** The fabrication of microfluidic devices to mimic lung microenvironment and physiology. **c** Application of lung-on-a-chip systems to evaluate respiratory diseases associated with contamination, smoking, infections, nanoparticles, drugs, etc.

an in vivo microenvironment that mimics functional living cells. The present review highlights various lung cell culture models and the ensuing development of the lung-on-a-chip device, its application in analyzing human respiratory diseases in vitro and existing challenges.

Developments in in vitro modeling of the human lung

Fabrication of an accurate representative lung model to represent in vivo functional and morphological aspects is the basic requirement for investigating pathogenesis in human lungs. In vitro models for respiratory disease have been modified over the years depending on complexity requirements. Studies of these models have reported the inclusion of single or multiple cell types, either originating from lung tissues or from multiple other organs, to establish the required physiological relevance.

2D culture models

Monolayer 2D culture or culturing cells at the air–liquid interface (ALI) are the most basic approaches and are practiced extensively for in vitro modeling of respiratory diseases. In 1999, Elbert et al. [25] reported in vitro culture of normal human lung tissue-derived human alveolar epithelial cells on collagen-I or fibronectin-coated polyester filter inserts. The cells proliferated well to form a confluent monolayer culture with tight junctions, reaching a TEER (transepithelial electrical resistance) value of (2108±62) $\Omega \cdot cm^2$ after 8 days of culture. Later, matrigel, an extracellular matrix (ECM)-associated protein gel secreted by Engelbreth-Holm-Swarm mouse sarcoma cells, was established as an effective material for coating glass coverslips or tissue culture plates to maintain alveolar type II (AT2) epithelial cells in two dimensions. However, in 2D cultures, AT2 cells acquire a flattened morphology which is different from their natural cuboidal shape, as experienced after only 24–48 h of culture. The AT2 cells also lose the ability to produce surfactant and characteristic lamellar bodies within only 3–5 days of culture [26]. Again, it is widely reported that AT2 cells, which are the resident stem cells of the lung, proliferate in response to lung injury and can differentiate into AT1 cells in conventional 2D cultures [27], so it is not possible to maintain functional AT2 cells in vitro. Another important approach for in vitro culture of lung epithelial cells which has been reported is the culture of cells in the air–liquid interface, which can promote differentiation of epithelial cells toward basal cells, club cells, goblet cells, and ciliated cells, thus closely mimicking the in vivo multicellular microenvironment [28]. Bluhmki et al. [29] reported the culture of human small-airway epithelial (hSAE) cells on collagen-I coated transwell membranes; they were maintained in an ALI condition for over four weeks. The

model culture gave a pseudostratified epithelium with multiple epithelial cell types (basal, club, goblet, and ciliated) and was responsive to profibrotic cytokines such as transforming growth factor β1 (TGF-β1) and tumor necrosis factor α (TNF-α). Furthermore, Xu et al. [30] reported that when maintained with both apical and basolateral feeding, i.e., away from the air–liquid interface, airway epithelial cells showed reduced oxidative metabolism compared to cells maintained with only basolateral feeding at the ALI. Thus, it can be concluded that ALI is superior to traditional 2D culture for lung epithelial cells for studying lung pathophysiology and is a more appropriate technique for fabricating an in vitro cellular microenvironment that mimics in vivo conditions.

Spheroid/organoid cultures

Multicellular spheroids or organoids from patient-derived cells can be used as a scaffold-free 3D microtissue model, which has been established as a valuable tool in developing personalized medicine [31, 32]. Lung spheroids can be formed from healthy cells or cancer cells by self-aggregation of the lung cells; the resulting lung spheroids better resemble the functional and morphological microenvironment found in vivo [33]. In this context, Cores et al. [34] proposed a robust and rapid method for fabrication of healthy human lung tissue-derived human lung spheroids, which showed progenitor markers, e.g., surfactant protein C (SFTPC) and club cell secretory protein (CCSP). They used suspension culture on ultra-low-attachment plates and were able to successfully apply the method for treatment of idiopathic pulmonary fibrosis in a rat model. Interestingly, the spheroids were further disaggregated when cultured on an adherent surface coated with fibronectin, and were applied as supporting cells along with the progenitor cells from lung spheroids to create a physiologically relevant in vitro culture model. Another group, Dinh et al. [35], used a similar approach to obtain human lung progenitor cell-based spheroids and lung spheroid cells from pulmonary tissues. These spheroid cells could have applications in cell-based therapies, especially for COPD, IPF, and other diseases. However, the most prominent application of lung spheroids discovered so far is in modeling lung adenocarcinoma (LADC), due to the technique's ability to preserve mutational and histological characteristics of the parental tumor [36]. Researchers have established many drug screening platforms with lung cancer organoids derived from patients at different clinical stages; for example, Li et al. [36] reported the establishment of 12 LADC organoid lines from various tumor resections. The organoids showed specific biomarkers, phenotypes, and molecular characterization comparable to those of the corresponding parental tumor tissue; thus, this method can be applied to obtain representative in vitro models for drug screening. The major challenges for application of spheroids for in vitro modeling of human lung tissue are variation in spheroid size, induced hypoxia due to scarcity of oxygen, nutrient transport to the core when spheroid size is more than 200 μm, and formation of small spheroids with less cell diversity [37].

Scaffold-based 3D cultures

The microenvironment plays an important role in the functional preservation of cells and can modulate the phenotype and genotype of cells while maintaining them in vitro. Scaffolds of natural or synthetic origin can provide a 3D microenvironment superior to 2D culture conditions to preserve organ-specific functions; they have proven efficacy for in vitro disease modeling and drug-screening applications (Fig. 2). Of various types of scaffolds, decellularized ECM (dECM) lung scaffolds have attracted more significant attention due to their preservation of the composition of major ECM proteins. Crabbé et al. [38] reported recellularization of decellularized mouse lungs with bone-marrow-derived mesenchymal stromal (stem) cells (MSCs) and AT2 cells in a bioreactor. The dynamic culture on dECM supported better cell viability and reduced apoptosis, thus making it suitable for long-term culture of functional AT2 cells. Although natural ECM-derived scaffolds provide excellent biological cues for cell attachment and growth, they usually possess inferior mechanical properties and exhibit faster enzymatic degradation and significant batch-to-batch variation [39]. Thus, scaffolds that combine both synthetic and natural ECM-derived polymers to provide the required mechanical properties along with biological cues have been fabricated and applied for lung-tissue engineering. Rezaei et al. [40] created a 4:1 chitosan-to-polycaprolactone scaffold suitable for culturing MRC-5 lung fibroblasts, which could be applied in lung tissue engineering. However, cells cultured on a 3D-printed scaffold provide a more 2D-like architecture, although the microenvironment they foster is mechanically and morphologically superior compared to conventional culture on tissue culture plastic (TCP). Wang et al. [41] addressed this challenge by 3D printing lung cancer cells A549/95-D as a suspension with a gelatin–alginate solution to form cell-laden hydrogels and were able to maintain the culture for 28 days. The 3D-bioprinted cells showed superior replication of the cancer microenvironment with enhanced capabilities of migration and invasion compared to conventional 2D models. Another group, Young et al. [42], mimicked the fibrous nature of native ECM structure by fabricating electrospun scaffolds from poly-L-lactic acid (PLLA) and decellularized pig-lung ECM (PLECM). In comparison with scaffolds made of only PLLA and both PLLA- and PLECM-coated tissue culture plates with no structural cues, the combined PLLA/PLECM spun scaffold was found to be superior for supporting human bronchial smooth muscle cells (HBSMCs), which acquired a contractile morphology

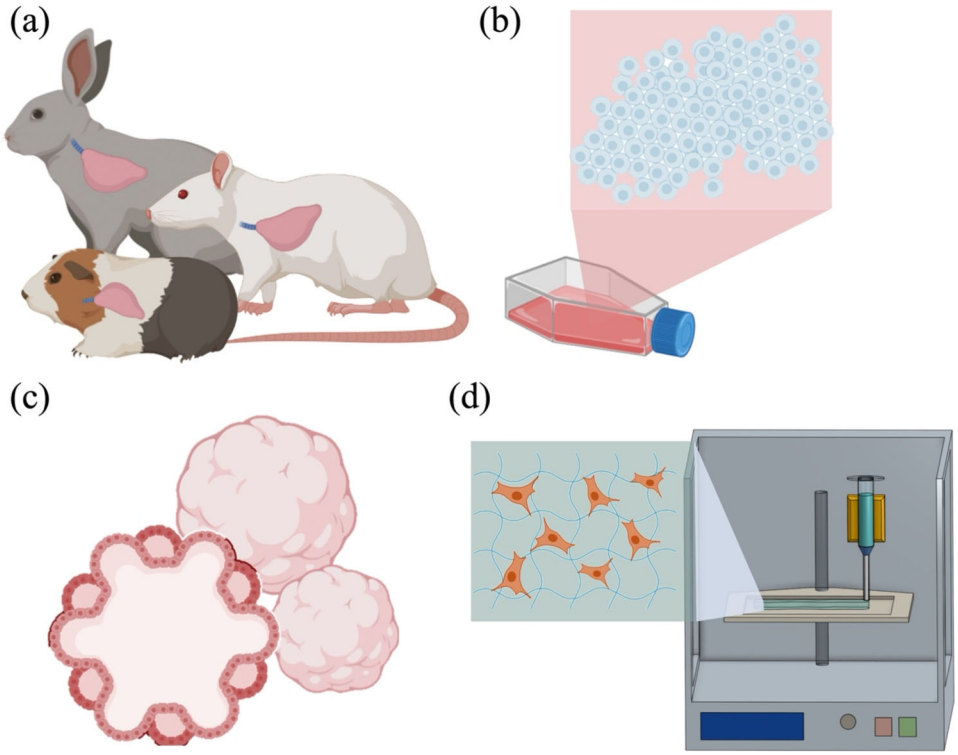

Fig. 2 Different models for lung research. **a** Animal models. **b** Cell monolayer. **c** Spheroid culture. **d** Scaffold-based 3D culture in biofabrication

and showed a significantly higher expression of alpha-1 type 1 collagen after one week of culture. Overall, 3D scaffolds with structural, morphological, and biological cues have been established as an improved model for in vitro analysis of lung pathophysiology in healthy and disease conditions, due to their advantages over the tested 2D culture models with inferior biophysical cues.

In conclusion, different technologies have been explored and analyzed over the past years for in vitro modeling of respiratory diseases. In 2017, Wan et al. [43] established that perfusion culture is a significant factor in effectively recapitulating the physiological conditions for maintaining lung cancer spheroids in vitro. These investigations lead us to the need to use dynamic culture to produce a more relevant cell microenvironment in vitro. Perfusion culture introduces a continuous physiologically relevant flow gradient of culture media and biologically active molecules into the culture chamber. It offers high spatial and/or temporal resolution of single cells and minimal circulation of a calculated amount of culture media [44]. The development and applications of these microfluidic perfusion culture models for analyzing lung pathophysiology are discussed in subsequent sections.

Microfluidics to model the in vivo lung microenvironment

Microfluidic organ-on-a-chip devices are cell-culture models that can recapitulate pivotal human organ architecture, function, and pathophysiology in vitro. They can be simple or structurally complex devices consisting of one or several chambers with microchannels [45] to provide embedded cells or tissues with nutrients, growth factors, drug compounds, or toxins in physiologically relevant concentrations. Microfluidic devices enable fluid manipulation at the micro-/nanolevel, which allows a constant temperature to be maintained. The continuous supply of medium also creates physiologically relevant shear flow and a chemical gradient, essential to reproducing processes and mechanisms that occur in vivo [46]. To recapitulate the physiological features of organs, cell–cell interactions, and cell–ECM communications, there is a valid need to integrate biophysical and mechanical cues into one device [47]. Lung-on-a-chip is a micro-engineered cell-culture platform developed to reproduce the critical biochemical, structural, functional, and mechanical properties of the human alveolar–capillary interface [48, 49]. Most lung-on-a-chip devices are fabricated in a 3D microchannel system, which consists of upper and lower cell-culture chambers separated by an ECM-coated microporous membrane. To produce an air−blood interface, alveolar epithelial cells and vascular endothelial cells are cultured on opposite sides of the porous membrane. After confluency, the epithelial compartment is introduced to the airflow. In 2010, Huh et al. [48] for the first time developed a microdevice to reproduce complex integrated organ-level responses to bacteria and inflammatory cytokines introduced

into the alveolar space. Two lateral microchambers were integrated alongside the cell chambers to induce stretch by cyclic vacuum; this mimicked physiological lung breathing movements. A co-culture of two types of cells was established on top of a thin, flexible, and porous polydimethylsiloxane (PDMS) layer and then perfused with a culture medium for up to two weeks. Another novel 3D human lung-on-a-chip model was proposed by Zhang et al. [47] to study the effect of inhalation of nanoparticles like TiO_2 and ZnO during pulmonary exposure. The proposed platform had three parallel channels for co-culture of human alveolar epithelial cells and endothelial cells, as well as a sandwiched Matrigel membrane layer to mimic the alveolar–capillary barrier. However, biological and mechanical cues such as stretch stress (to mimic lung movement) were not integrated into this chip. To show the impact of mechanical strain induced by breathing, Stucki et al. [50] designed a lung-on-a-chip array integrated with a micro-diaphragm to stretch the alveolar barrier. They showed that the permeability properties of the epithelial cell monolayer, metabolic activity, and the cytokine secretion of patient-derived primary human alveolar epithelial cells were significantly influenced by cyclic stretching of the alveolar barrier. Another group, Zamprogno et al. [51], developed a device to mimic the breathing movement in the air–blood barrier and to reproduce the characteristics of the alveolar network, along with biochemical and biophysical properties of the alveolar basal membrane. The proposed lung-on-a-chip device was fabricated by using a stretchable and biodegradable membrane made of collagen and elastin to reproduce an array of tiny alveoli of similar size, as observed in vivo. The reported membrane outperforms PDMS in many ways, such as ease of fabrication, biodegradability, and prevention of rhodamine-B absorption. However, these first-generation lung-on-a-chip devices imperfectly reproduce the geometric dimensions of the native lung alveoli, as the surface of the culturing membrane creates a unique alveolus of non-physiological dimensions rather than an array of alveoli with in vivo-like anatomy. In the most recent generation, the structure of the alveolus has been taken into consideration. For instance, the average diameter of each natural alveolus is about 200 μm. The recent lung-on-a-chip models reflect these dimensions by incorporating porous structures with diameters around 200–260 μm [51, 52]. Future efforts are expected to concentrate on mimicking the alveolar walls with their capillary networks, connective tissue, and parenchymal construction.

For example, Huang et al. [53] presented a relevant model of human pulmonary alveoli on a chip. The platform was composed of a compartmentalized PDMS chip to deliver a medium supply, form an air–liquid interface, and apply cyclic strain to a 3D porous hydrogel made of gelatin methacryloyl (GelMA), with an inverse opal structure containing primary human alveolar epithelial cells (hAECs). The cyclic stretch applied to the GelMA construct produced an expansion of about 8% in the average size of the 3D formed alveoli from the state of "breath out" to "breath in." This is comparable to the 5% to 15% range of physiological strain experienced by the alveoli in the human lung.

Another gain that emerged from developing organ-on-a-chip devices was the integration of sensors, which are critical in continuously measuring the microenvironmental parameters and the dynamic responses of microtissues to pharmaceutical compounds in real time [53]. In recent decades, key parameters such as TEER, which quantifies the tightness of junctions or cellular barriers, have been examined with regard to their activity in transporting drugs or chemicals [54]. To date, most of these studies [55–59] have utilized commercial systems such as EVOM2 or Millicell ERS to measure TEER values. However, integrating sensors into a microfluidic platform provides a non-invasive real-time measurement for continuously monitoring the development and performance of the epithelial barrier upon treatment with drugs or toxins on-chip. Henry et al. [57] developed a microfluidic organ with embedded electrodes to assess the formation and disruption of barrier function within a human lung-airway chip lined with fully differentiated mucociliary human airway epithelium. They also demonstrated the ability of the microfabricated device to measure barrier function with virtually any type of cultured cells by monitoring the TEER values in a human gut-on-a-chip lined with intestinal epithelial cells. Another group, Mermoud et al. [60], designed a micro-impedance tomography (MITO) system integrated into a lung-on-a-chip device to monitor the electrochemical and mechanical changes occurring in the lung alveolar barrier due to breathing movement, using impedimetric coplanar electrodes. Integration of electrodes provides the ability to continuously monitor resistivity changes related to lung alveolar barrier integrity, as well as deflection of the barrier that occurs with breathing movement. In another study, Skardal et al. [61] reported a body-on-a-chip system that integrated more complex bioengineered liver and cardiac tissue organoids in perfusable devices that were connected to a lung organoid at the air–liquid interfaces. Custom trans-epithelial electrical resistance electrodes were integrated into the lung module for real-time monitoring of organoid integrity and changes in functions including ion-channel activity, which is critical for lung function. Although there is still much scope for further improvement in lung-on-a-chip models, it is already an advanced technology for analyzing respiratory disease and rapidly screening drug libraries. Recent relevant applications of lungs-on-a-chip are summarized in Table 1.

Table 1 Synoptic table of various recent applications of lungs-on-a-chip

Lung-on-a-chip application	Physiological parameter of interest	Cell distribution (2D or 3D)	Cell type	Mechanical stimulus	Parameter to investigate	Reference
COVID-19	Penetration of alveolar–capillary barrier by virus-like particles	2D/3D culture	hAECs	Liquid flow and vacuum	IL-8, IL-6, IL-1β, MCP-1, and GM-CSF	[53]
Alveolar stretching	Alveolar distribution and shape	2D culture in elastin and collagen	hAEpCs	Liquid flow, vacuum	E-cadherin, ZO-1	[51]
Air pollution	Alveolus inflammation	2D culture	HPAEpiCs and HPMECs	Air–liquid interface and liquid flow	IL-6, IL-8, MCP-1, IP-10, GM-CSF, RANTES, IL-1β, G-CSF, TNF-α, and IL-12	[62]
Pulmonary fibrosis	Idiopathic pulmonary fibrosis	2D and 3D culture	NHLF, iPF-HLF, HUVECs, SAECs	Liquid flow	ZO-1, αSMA, Tubb4, CC10	[63]
Lung cancer	Tumorigenesis	3D culture in collagen matrix	ECs, 3T3, A549	Liquid flow	IL-6, VEGF, TP53I3, AGT, CXCL2, etc.	[64]
Lung cancer	Metastasis	3D culture in GelMA	A549, NHLF	Air–liquid interface and liquid flow	IL-6, αSMA, ZO-1	[65]
Lung cancer	Cell apoptosis	2D culture	NCI-H1437	Liquid flow	Real-time measurement of pH, TEER	[66]
Pulmonary arterial hypertension (PAH)	Sex discrepancy of PAH	2D culture	PACs, endothelial, smooth muscle, and adventitial cells	Liquid flow	ColT1, aromatase, and CYP1B1	[67]
Drug toxicity	Lung–liver homeostasis	2D culture	Bronchial cells	Liquid flow, airway interface	pO2, TEER, and ATP	[68]

GelMA: gelatin methacryloyl; hAECs: human amnion epithelial cells; hAEpCs: human alveolar type I-like cells; HPAEpiCs: human pulmonary alveolar epithelial cells; HPMECs: human pulmonary microvascular endothelial cells; NHLF: normal human lung fibroblast; iPF-HLF: idiopathic pulmonary fibrosis human lung fibroblast; HUVECs: human umbilical vein endothelial cells; SAECs: human small-airway epithelial cells; ECs: endothelial cells; PACs: pulmonary arterial cells; GM-CSF: granulocyte–macrophage colony-stimulating factor; MCP-1: monocyte chemoattractant protein-1; IP-10: interferon gamma-induced protein 10; RANTES: regulated upon activation, normal T cell expressed and secreted; αSMA: α-smooth muscle actin; ZO-1: tight junction protein-1; TNF-α: tumor necrosis factor alpha; TEER: transepithelial electrical resistance; Tubb4A: tubulin beta-4A; CC10: club cell protein 10; TP53I3: tumor protein P53 inducible protein 3; AGT: angiotensinogen; CXCL2: chemokine (C-X-X motif); ColT1: human coactosin-like 1; CYP1B1: cytochrome P450 1B1

Application of lung-on-a-chip models

Disease modeling

Modeling of air pollution-associated lung disease

Air pollution leads to multiple respiratory diseases, starting from minor airway irritation and progressing to inflammatory responses which can further result in cell apoptosis [69, 70]. The biomechanical and physiological features of lung tissues are explored in micro-engineered models to analyze environmental pollution-induced respiratory illness. Zhang et al. [71] designed a microphysiological system including a chemical gradient of benzopyrene to study the real-time effect of environmental pollution. They studied inflammation-associated lung injury in bronchi up to a single-cell resolution (Fig. 3a). In this model, the fabricated microfluidic system was composed of two layers: a channel network (microfluidic/gradient generator) and a cell chamber array. To investigate inflammatory responses to environmental pollutants, they established a monoculture of the human bronchial epithelial cell line

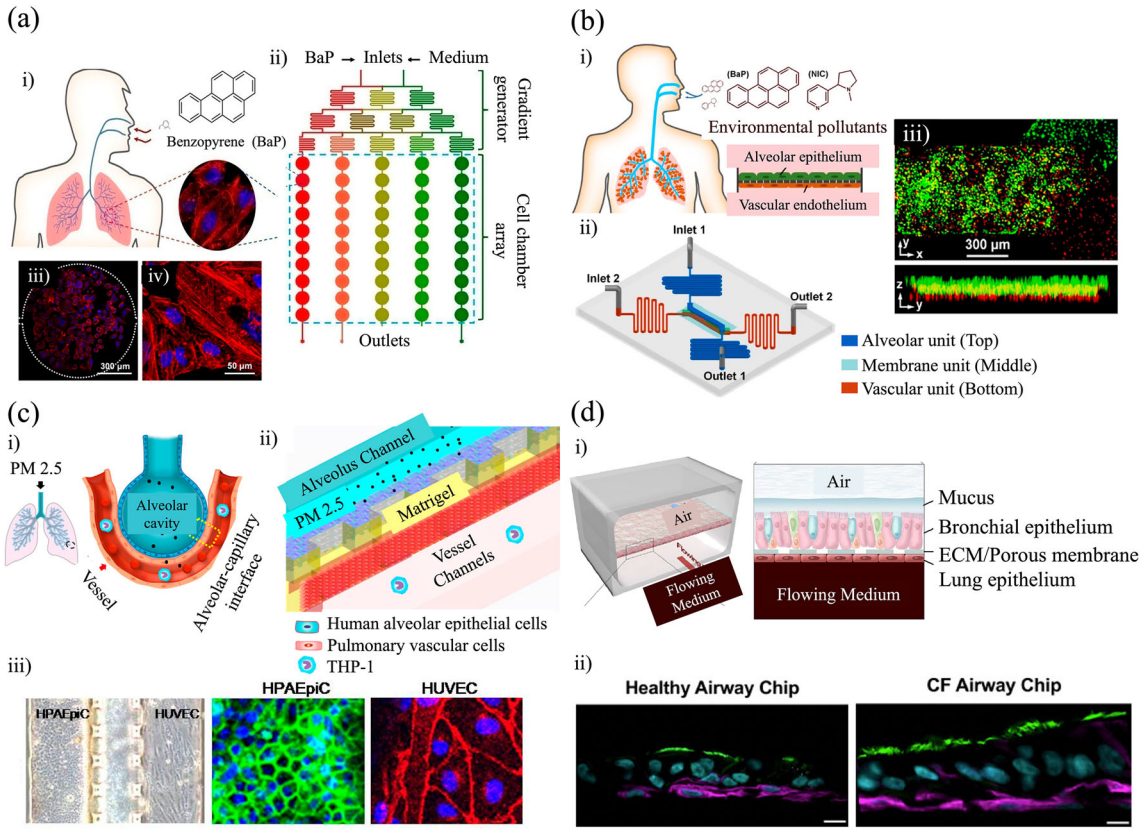

Fig. 3 Applications of the lung-on-a-chip for disease modeling. **a** Microfluidic device for environmental pollutant assays. The 16HBE cells of the bronchial epithelium were cultured and exposed to (i) benzopyrene to produce inflammatory injury in (ii) a microfluidic gradient generator device. (iii) Fluorescence image of actin (red) and nucleus (blue) staining for cytoskeletal evaluation of the cultured bronchial epithelium. (iv) Enlarged image of the actin-filament (red) and nucleus (blue) staining. Reproduced from [71], Copyright 2018, with permission from American Chemical Society. **b** Co-culture of double tissue interface to (i) evaluate inflammation and injury under polluted conditions. (ii) Microfluidic device including alveolar, membrane, and vascular units. (iii) Fluorescence visualization of epithelial (green) and endothelial cells (red) in both planar and vertical sections. Reproduced from [62], Copyright 2020, with permission from American Chemical Society. **c** Fine-particle pulmonary exposure model, (i) representation of pulmonary PM2.5 exposure in vivo. (ii) Model of pulmonary PM2.5 exposure on the lung-on-a-chip. Human alveolar epithelial cells (HPAEpiC) and endothelial cells (HUVECs) are co-cultured. (iii) Bright-field micrographs of HPAEpiCs and HUVECs after three days of culture in the microfluidic device (scale bar: 200 μm); fluorescence images of HPAEpiCs stained with E-cadherin and DAPI; and fluorescence images of HUVECs with VE-cadherin and DAPI (scale bar: 30 μm). Reproduced from [72], Copyright 2020, with permission from American Chemical Society. **d** Lung cystic fibrosis (CF) microfluidic model. (i) Diagram of the device showing the pseudostratified bronchial epithelium and vascular channel. (ii) Immunofluorescence images of vertical cross-sections of healthy and cystic fibrosis chips, showing ciliated cells expressing β-Tubulin IV (green) and basal cells expressing CK5 (magenta) (scale bar: 10 μm). Reproduced from [73], Copyright 2021, with permission from European Cystic Fibrosis Society

(16HBE). By monitoring real-time Caspase-3 activation, they were able to demonstrate that benzopyrene impacts bronchial epithelium cell morphology by causing cytoskeleton disintegration. The system also successfully assessed the upregulated production of reactive oxygen species (ROS) and detected released inflammatory cytokines (e.g., TNF-α, IL-6, and IL-8). In follow-up research, Zhang et al. [62] also studied lung inflammation and injury in an alveolar–epithelium and microvascular endothelium co-culture model. The mechanical and functional properties of epithelium–endothelium interfaces were also incorporated in this system by using a double tissue layer. Human pulmonary alveolar epithelial cells (HPAEpiCs) and human pulmonary microvascular endothelial cells (HPMECs) were co-cultured on the top and bottom side of the tissue layer, respectively. The HPMECs were exposed to medium flow, and the HPAEpiCs were stimulated by pollutant flow. Inflammatory signals (i.e., reactive oxygen species and cytokines), as well as apoptosis and cytoskeleton stability, were studied in this model. The group demonstrated that environmental pollutant-induced inflammatory injury of an alveolus could be replicated in this biofabricated microphysiological system (Fig. 3b). In this study, the effects of small particle size contamination (<2.5 μm) on lung disease were analyzed and proved to be

associated with higher morbidity and mortality. In another study, Xu et al. [72] proposed a lung-on-a-chip model to evaluate the potential risk of fine particles at the alveolar–blood barrier level; they used a culture of human epithelial cells along with ECM proteins. The microfluidic system was composed of representative human lung alveolar epithelial cells and matrigel to emulate the ECM between the epithelium and endothelium. Human umbilical vein endothelial cells (HUVECs) were also included in the model to represent the vessel side of the alveolus. Particles <2.5 μm in size were applied to the channels lined with lung epithelial cells to emulate pulmonary exposure to fine particles (Fig. 3c). The results indicated that high doses of microparticles can lead to adherence junction disruption on alveolar–capillary barriers. This phenomenon also results in upregulation of ROS generation, cell apoptosis, elevated permeability, and monocyte attachment.

Smoking

Cigarette smoke is a major cause of lung pathogenesis and reportedly results in 29% of cancer-related deaths worldwide [74]. To date, many platforms have been proposed to determine the pathogenesis and mechanisms of cigarette smoke-induced injury in lung tissues. Shrestha et al. [75] presented a rapidly prototyped lung-on-a-chip model to successfully evaluate the effect of cigarette smoke extract on lung cells in vitro. This group introduced a model fabricated by mold-casting PDMS, to simplify the fabrication process. The microfluidic device has an open-well design that was capable of dynamically simulating the airway and air–liquid interface. Calu-3, a human non-small cell lung cancer (NSCLC) cell, was cultured over an ECM protein-coated polycarbonate membrane. The model demonstrated that Calu-3 replicates the 3D culture-specific morphology by maintaining excellent barrier integrity and mucus secretion, as well as successfully expressing the cell-surface functional P-glycoprotein. To validate the microfabricated system, cells were exposed to cigarette-smoke extract (CSE), which resulted in the production of inflammatory cytokines such as interleukin-6 (IL-6) and interleukin-8 (IL-8). The administration of CSE decreased expression of E-cadherin (E-Cad) and resulted in disruption of the epithelial barrier. Finally, application of budesonide, an anti-inflammatory steroid, attenuated the impact of CSE on Calu-3. Notably, this research presents a simple and effective strategy for fabricating microfluidic devices. COPD is one of the main consequences of chronic smoking. It is a progressive respiratory disease that can potentially affect the functional activities of the human lung due to chronic pulmonary inflammation, airway thickening, and loss of alveoli [76]. Hou et al. [77] designed a smoking-induced COPD model by mimicking the carcinogenesis of epithelial tissues. They fabricated a breathing lung, including vascular endothelial and bronchial epithelial cells, to mimic the microenvironment of the air–blood interface. To trigger inflammation, cells were exposed to CSE at concentrations of 10, 20, and 50 μg/mL. The secretion of inflammatory cytokines, including IL-6 and tumor necrosis factor-alpha (TNF-α), was measured for each concentration of CSE. The group observed that exposure to CSE can induce degradation of the apical junction complex and activate phosphorylation of proto-oncogene STAT3; this promotes the epithelial-to-mesenchymal transition (EMT) and accelerates cell division, resulting in a tumor-like transformation. However, the system involved a complex fabrication process. Also, the in vivo 3D alveolus structure was simplified to a 2D structure, which could potentially cause misleading assessments of disease conditions.

While many research approaches oversimplified smoking exposure by introducing cigarette-smoke extract, very interesting work has been reported by Benam et al. [78, 79] in which a biomimetic smoking robot was coupled with a lung-on-a-chip platform. The smoking robot was capable of introducing fresh smoke from burning cigarettes to an epithelium-lined microchannel during inhalation, followed by exhalation in a cyclic pattern. This approach was used to mimic the real smoking scenario in the human lung. The integration of accurate physiological mechanical cues was accomplished by shear stress and cyclic strain. A physiologically relevant amount of smoke was introduced into the system and the effects were studied. The instrument was able to provide the smoke of nine cigarettes (over a period of 75 min) into the human multiciliate bronchiolar epithelium under physiological breathing conditions. The researchers reported an about tenfold increase in expression of an antioxidant gene (HMOX1), along with enhancement of phosphorylation of the oxidation-induced cytoprotective transcription-factor protein Nrf2, upon treatment with cigarette smoke. Finally, a genome-wide gene microarray analysis comparing acute exposure results against those obtained from pathology samples obtained during bronchoscopy from human smokers showed quantitative similarities between expressed genes associated with the oxidation–reduction pathway [80].

Pulmonary fibrosis

Application of lung-on-a-chip systems in the pharmaceutical industry has the potential to accelerate the drug-discovery process and to be adopted in high-throughput systems as required. Pulmonary fibrosis is produced by the continuous replacement of healthy alveolar tissue with scar tissue, thus resulting in chronic impairment of gas exchange and reduced lung compliance [81]. To study organ-level pulmonary fibrosis in vitro, Mejías et al. [63] proposed a micro vascularized human lung-on-a-chip platform using a 96-well

plate format to model fibrosis in the human lung interstitium–airway interface. This model facilitates fabrication, handling, and integration of the system by automated imaging platforms. The microfluidic device recapitulates the ALI of the lower respiratory airways by encapsulating normal or diseased fibroblasts within a fibrin–collagen hydrogel and placing them in the two lateral channels. In the central vasculature channel, HUVECs were seeded and later examined for TGF-β1 (0–10 ng/mL) diffusion. Normal human small-airway epithelial cells (SAECs) were seeded in the top air channel. The group successfully achieved air–liquid epithelial formation by evaluating the expression of beta-tubulin 4 and ZO-1 in the vascularity epithelium, using fluorescence microscopy. Also, a fibrotic pulmonary microenvironment was established, as evident from the upregulated expression of α-smooth muscle actin (α-SMA) in fibroblasts; changes were observed in uteroglobin expression in club cells and Tubb4 expression in the airway epithelium.

Another source of lung fibrosis is genetic disease. For example, cystic fibrosis (CF) is caused by mutations in the gene-encoding cystic fibrosis transmembrane conductance regulator that may lead to a reduction in mucociliary production and also can cause inflammation in the respiratory airway. Ratjen et al. described the increase in the risk of infections which may lead to respiratory insufficiency due to cystic fibrosis [82]. The development of new therapeutics to treat CF requires appropriate micro-physiological systems that include the complex interactions among epithelial, endothelial, and blood components in the lung airway. Plebani et al. [73] reported a cystic fibrosis-associated lung-on-a-chip model that incorporated patient-derived primary bronchial epithelial cells (HBE) and interfaced with primary human lung microvascular endothelium. The model recapitulated structural, biochemical, and pathophysiological features of cystic fibrosis (Fig. 3d) in lung tissues [68, 73]. The system was investigated for the presence or absence of polymorphonuclear leukocytes and *Pseudomonas aeruginosa,* which was applied as a bacterial pathogen. The CF chip successfully recapitulated mucus accumulation, showed increases in cilia density, and exhibited a higher ciliary beating frequency than healthy bronchial epithelial chips. Nonetheless, the CF chips secreted higher levels of IL-8, followed by enhanced adhesion of polymorphonuclear leukocytes to the endothelium and progressive transmigration to the airway compartment.

Lung cancer

Lung cancer is the most widely reported cause of cancer-associated deaths in the world (about 1.8 million in 2020) [3]. Many microphysiological systems have been developed to date to focus on improving 3D in vitro cancer models [46]. Lee et al. [64] presented a microfluidic model designed to confirm the role and function of various stromal cells in tumorigenesis. In this model, the cancer cells were cultured in a microfluidic channel that provided close interaction with the tumor microenvironment (Fig. 4a). To achieve this, endothelial cells, fibroblasts, and lung cancer cells were seeded and co-cultured within a collagen matrix. The microfluidic device was designed as a vessel-like flow channel through which a continuous flow of culture medium was introduced. The cells were seeded in multiple U-shaped wells. The results indicated that transforming growth factor-β (TGF-β), matrix metalloproteinase (MMP), and the biophysical forces generated by fibroblasts can induce tumor formation. Also, due to the introduction of fibroblasts in the co-culture system, the group reported upregulation of metastasis-associated genes and angiogenesis, and downregulation of apoptosis-related genes. Finally, the model was successfully challenged by introducing chemotherapeutic drugs, i.e., paclitaxel and gemcitabine, in lung cancer cells. Recently, we reported an all 3D printed in vivo mimicking 3D lung cancer-on-a-chip (IVM3DLCOC), which involves co-culturing lung cancer cells (A549) with normal human lung fibroblasts (HLFs) embedded in 3D hydrogels with similar surface hardness to human lung tissues. The microfluidic device includes an air channel connected to a porous membrane on the top of the lung epithelial cells, to emulate exhalation/inhalation cycles. The model was challenged and characterized in two scenarios: disease progression (i.e., metastasis) and drug efficacy. In the context of disease progression studies, we examined the exacerbation effect of cigarette-smoke extract on lung cancer cells. Our results showed preservation of metastatic characteristics (N-Cad, etc.) along with translational properties (IL-6, metastasis marker) of the human lung cells on the in vivo mimicking microfluidic lung model. As the second model of study, we carried out dose-dependent drug efficacy testing by monitoring the viability of the model cells in response to a model chemotherapeutic drug named paclitaxel. The results validated our model both for effectively studying the metastatic effect of cigarette smoke in human lung cancer cells and for drug screening for respiratory diseases. We envision the application of patient-derived healthy lung primary cells and primary tumor cells, along with stromal cells, to study the effect of external stimulus on the progress and inhibition of lung cancer in order to more closely model in vivo event cascades [65].

The importance of real-time monitoring [85–90] of lungs-on-a-chip might simplify the assessment of preclinical drug candidates. For example, Khalid et al. [66] presented a glass-based microfluidic chip in which a cell reservoir with two channels was 3D-printed with silicone ink [91–93]. The system was integrated with a non-invasive optical pH sensor, a TEER impedance sensing modulus, and a dedicated digital fluorescence microscope. The lung cancer-on-a-chip was

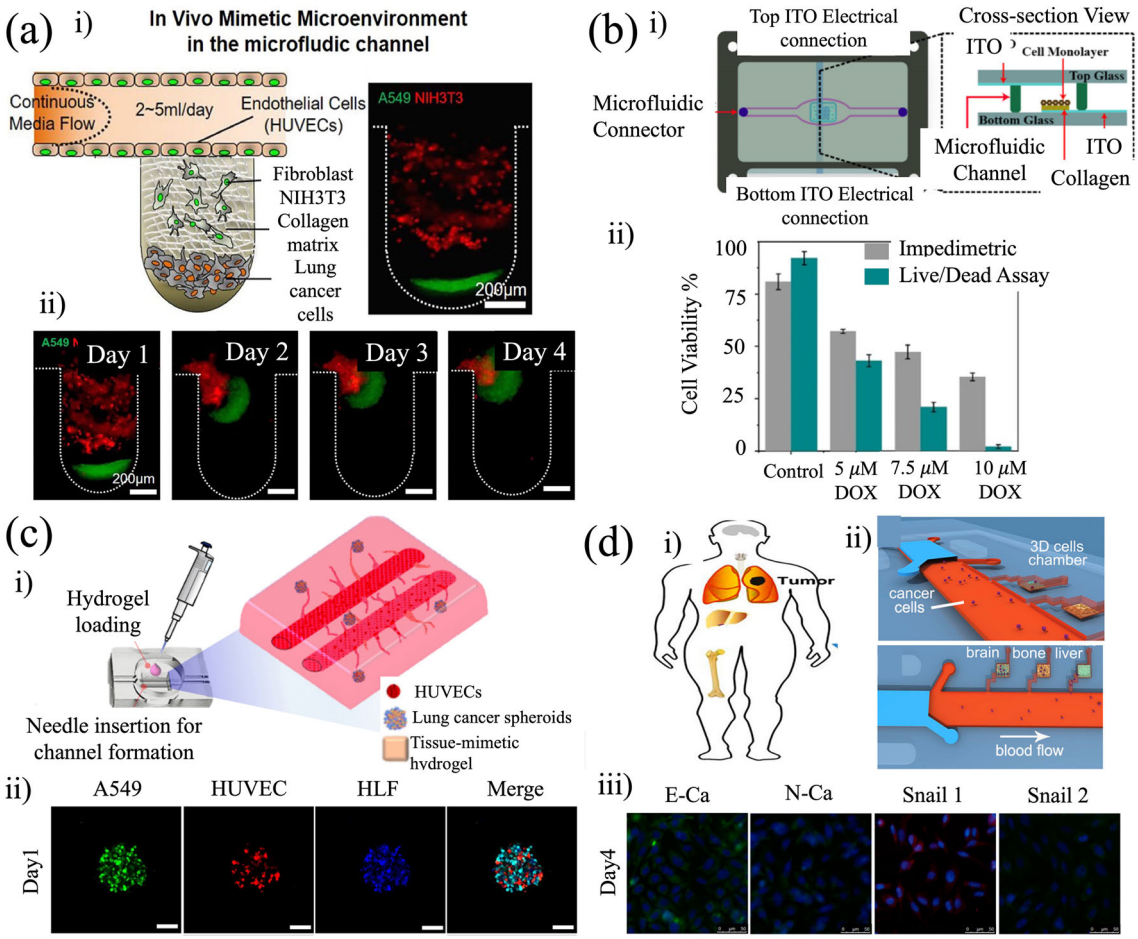

Fig. 4 Lung-on-a-chip applications in cancer. **a** Fibroblast tumor microenvironment. (i) Rational for mimicking the in vivo tumor microenvironment with vasculature, lung cancer cells, and fibroblasts, in which biophysical cues affect tumorigenesis and angiogenesis; (ii) formation of lung tumor spheroids between days 1 and 4. Reproduced from [64], Copyright 2018, with permission from the authors. **b** Integrated biosensors for physiological monitoring. (i) Schematic assembly of a microfluidic chip for real-time monitoring of deteriorating effects of chemotherapy in lung cancer cells; (ii) comparison of endpoint impedimetric and live/dead viability assays. Reproduced from [66], Copyright 2019, with permission from Elsevier. **c** Vascularized lung cancer-on-a-chip. (i) Lung cancer-derived tumor spheroids were encapsulated in a hydrogel to simulate the lung cancer tissue microenvironment. Two cylindrical channels with a diameter of 500 μm were endothelialized with human umbilical vein endothelial cells (HUVECs) inside the matrix to mimic perfusable large-sized vessel structure; (ii) fluorescence image of tri-cellular spheroids on Day 1 after seeding (scale bar: 100 μm). Reproduced from [83], Copyright 2021, with permission from the authors. **d** Lung metastasis-on-a-chip; (i) mock figure of lung cancer metastasis to multiple organs; (ii) schematic illustration of multiple organs on a chip, with a lung tumor and three downstream distant organs. (iii) A549 lung cancer cells expressed E-cadherin (green), N-cadherin (green), Snail1 (red), and Snail2 (green) after 4 days of culture on the microfluidic chip. Reproduced from [84], Copyright 2016, with permission from American Chemical Society

used to monitor the viability of NCI-H1437 lung cancer cells in real time under treatment with docetaxel and doxorubicin at concentrations of 0.1, 0.3, 0.5 nmol/L, and 5, 7.5, 10 μmol/L, respectively. The pH sensor showed extracellular acidification due to increased cell death. Fluorescence microscopy and impedimetric access showed upregulated cell death upon treatment with docetaxel. Also, the effect of docetaxel on cell viability was found to be more adverse in comparison with the effect of doxorubicin. Similar cell viability patterns were reported as evaluated by impedance measurement and live/dead assays, thus proving the usefulness of the microfabricated microfluidic platform for toxicity studies (Fig. 4b). Notably, this system successfully showed the effective application of integrated sensors inside the microfluidic devices for real-time monitoring of pH.

The incorporation of vascular networks into lung-on-a-chip platforms is a crucial step to overcoming the diffusion limitation and enabling the use of large tissue constructs [94]. Recently, Park et al. [83] developed a 3D vascularized lung-on-a-chip model to study lung cancer in vitro. In this model, decellularized lung extracellular matrix was

used as a scaffold to encapsulate tri-cellular spheroids made of A549 cells, HUVECs, and HLFs. To mimic perfusable vessels, two channels were incorporated into the hydrogel. Doxorubicin (Dox) was perfused into the microfluidic channels at concentrations of 1 and 5 μmol/L to elucidate a more effective dose-dependent response in the lung cancer model when compared with the corresponding 2D cell culture (Fig. 4c). Fluorescence microscopy images showed the maturation and growth of the endothelial network. Furthermore, the effective delivery of Dox with a significant dose-dependent variation was proved by live/dead and p53 enzyme-linked immunosorbent assays (ELISA). Nonetheless, Dox exhibits an anti-angiogenic effect in HUVECs. This approach could evolve to take advantage of decellularized ECM by incorporating patient-derived cells.

Another leading cause of enhanced mortality in lung cancer patients is cancer metastasis to distant organs. This synergistically enhances the need to establish a representative lung-on-a-chip platform with complex conditions that mimic in vivo disease [95]. Lung cancer usually metastasizes to the bone, brain, and liver, resulting in a poor prognosis. To mimic these conditions, Xu et al. [84] proposed a multi-organ micro-physiological system to recapitulate lung metastasis to the brain, bone, and liver. Bronchial epithelial (16HBE), lung cancer (A549), endothelial (HUVEC), and lung fibroblast (WI 38) cells were co-cultured, while astrocyte (HA-1800), osteoblast (Fob1.19), and hepatocyte (L-02) cell lines were cultured as distant organs to closely mimic and analyze the metastatic conditions. The system was conceived by reconstituting lung cancer migration while co-cultured with stromal cells to induce cancer migration and by injecting solutions to mimic hematogenous metastasis. The co-culture with cancer cells led to a transformation of fibroblasts and macrophages toward cancer-associated fibroblasts (CAFs) and cancer-associated macrophages (CAMs) (Fig. 4d). Physico-chemical transformations in brain, bone, and liver cells due to the metastasis of lung cancer cells were also evident in the overexpression of damage-associated markers such as C-X-C chemokine receptor type 4 (CXCR4) in astrocytes, receptor activator of nuclear factor kappa-B ligand (RANKL) for osteocytes, and alpha-fetoprotein (AFP) in hepatocytes. The platform enables analysis and visualization of complex cell behaviors such as expression of epithelial and stromal cell markers. For instance, co-culture of A549 lung cells with astrocytes, osteocytes, and hepatocytes resulted in overexpression of CXCR4, RANKL, and AFP, respectively, indicating damage to these healthy cell types. Thus, the model effectively proved its applicability for studying lung cancer metastasis to distant organs.

Asthma

Worldwide, around 300 million people have asthma [96]. Current information suggests that asthma is a multifactorial disorder, and its etiology is related to genetic susceptibility, host factors, and environmental factors [97]. The pandemic caused by SARS-CoV-2 also attracted significant attention to asthma patients because asthma can manifest as a major pathological condition and worsen the viral effect on the respiratory system [98]. However, the complex mechanism of asthma exacerbation is still under investigation. In this context, Nawroth et al. [99] reported a micro-engineered model of rhinovirus-induced asthma exacerbation, mimicking viral infection of airway epithelium and neutrophil migration. The microfluidic devices consist of three main components that include top and bottom PDMS chambers which remain separated by a porous (pore size: 3 μm) polyester (PET) membrane. Human primary airway epithelial cells and HUVECs were co-cultured on the top and bottom chambers, respectively. To induce the asthmatic phenotype in the human airway epithelium, interleukin-13 (IL-13, 100 ng/mL) was perfused for 7 days in the micro-engineered system. This approach resulted in hyperplasia in goblet cells, caused a reduction in cilia beating frequency, and also contributed to endothelial activation, which is the major pathogenesis commonly found in asthmatic epithelium. In addition, to mimic viral infection and exacerbation, rhinovirus strain 16 was inoculated on the chip after asthma induction. To study the inflammatory effect of viral infection, IL-6, IL-8, and cytokines were monitored. The results showed upregulated secretion of interferons (IFNs) and IFN-induced chemokines. Also, the group observed that secretion of IL-8 was increased after 48 h of infection, while IL-6 secretion was reduced. The data suggest that IL-13 may impair the host's ability to show a normal immune response toward rhinovirus infection. The results thus confirmed the capability of this model to replicate key biochemical features of asthma cytopathology.

Inflammation

Pulmonary inflammation is an organ-level process governed by complex tissue–tissue interactions between the lung epithelium and the microvascular endothelium that regulates immune response during respiratory pathogenesis, sepsis, allergic reaction, and trauma [100]. Benam et al. [101] developed an inflammation model of a human small airway-on-a-chip incorporating mucociliary bronchiolar epithelium and microvascular endothelial cells exposed to fluid flow. Modeling of human lung inflammation was achieved by administration of IL-13, which promoted hyperplasia in goblet cells, along with cytokine hypersecretion, and resulted in decreased ciliary function in situ.

Another pulmonary-inflammation biomimetic system was proposed by Punde et al. [102]; it sandwiches a micropore-array silicon chip between two PDMS channels. The bronchial epithelial Beas-2B cells were cultured on the fibronectin-coated micropores. Eosinophil cationic protein (ECP) was administered to induce inflammation in this culture model. ECP was found to stimulate migration of fibrocytes toward the epithelium by secretion of CXCL-12. This migration disturbs the surfactant function of the alveolus. The model uses a human bronchial epithelial cell line (Beas-2B) infected with adenovirus and co-cultured with circulating human fibrocytes. Administration of 5 mmol/L ECP for 3, 6, 12, and 24 h resulted in overexpression of CXCL-12 by 1.7-, 3.5-, 4.7-, and 2.6-fold, respectively. The increase in CXCL-12 expression leads to migration of fibrocytes toward Beas-2B cells. This platform demonstrates the influence of the CXCL12-CXCR4 axis in mediating fibrocyte extravasation in lung inflammation. The model mimicked the influence of ECP on lung inflammation by providing a dynamic migration tool.

Pulmonary hypertension

Pulmonary arterial hypertension (PAH) is a condition characterized by elevated pulmonary arterial pressure, caused by an increase in the stiffness of artery walls. Thus, in compensation the heart must work harder to pump blood through occluded arteries into the lungs for oxygen exchange. The heart's effort to work harder can cause enlargement, which can then lead to heart failure and mortality. The etiology comes from the aberrant proliferation and migration of pulmonary arterial cells, followed by enhanced deposition of extracellular matrices [103]. Recently Al-Hilal et al. [67] reported a microfluidic device to study the sex discrepancy in PAH by mimicking the luminal, intimal, medial, adventitial, and perivascular layers of a pulmonary artery using patient-derived cells. Three types of cells, including pulmonary arterial cells (PACs) and endothelial, smooth muscle, and adventitial cells, were included in this model. It was observed that cells derived from male patients developed more severe disease compared to those derived from female patients. Also, a greater elevation in the thickness of intimal and medial layers, induced by β-Estradiol, was reported for the chips with female patient-derived cells. Finally, the study also discussed the fact that the device can react to sex hormones much like real patients do. This study demonstrated the capacity of the customized microphysiological system for developing sex- and age-specific models for pulmonary hypertension. It could thus be an emergent technology for developing personalized medicine (Fig. 5a).

Wound healing

After acute and chronic respiratory disease, lungs can experience a remodeling process. Idiopathic pulmonary fibrosis (IPF), a chronic and fatal lung disease that is associated with micro-injuries in the alveolar epithelial tissues, can result in abnormal wound healing [106]. Felder et al. [106] reported a micro-engineered lung-on-a-chip with a breathing membrane, for studying the influence of cyclic mechanical stress during the alveolar wound repair process. For this purpose, lung alveolar epithelial cells were cultured until confluence over an ultra-thin elastic membrane and then wounded by scratching with a micropipette tip. The wound healing process was investigated for 24 h under the influence of multiple concentrations of recombinant human hepatic growth factor (hHGF) and mechanical stretching. The observations proved that mechanical stretch could impair the wound healing process in the alveolar epithelium (Fig. 5b).

Use of mechanical ventilation in patients with pulmonary deficiencies may produce overdistension and injuries in lung epithelia because of excessive pressure [107]. Tas et al. [104, 108] recently reported a lung-on-a-chip model that mimics a ventilator-induced lung injury. The model is composed of a nanofibrous synthetic membrane of poly(caprolactone) placed on a PDMS microfluidic device. Murine lung alveolar epithelial cells were seeded over the nanofibrous membrane, which was subjected to a rhythmic mechanical stress of 0.1 Hz along with rhythmic motion, using a flow rate of 108 mL/h for 2 h to induce wound formation on the alveolar epithelial cells. Applied mechanical stretching resulted in cellular injury, confirmed by an elevated concentration of lactate dehydrogenase (LDH). The stretch also caused cellular changes in YAP/TAZ mechanotransducers (Fig. 5c).

Thrombosis

Pulmonary thrombosis begins with the activation of platelets. Inflammatory stimulation of the lung vascular endothelium leads to the formation of thrombi, which is a major cause of mortality in multiple lung diseases [109]. Jain et al. [105] proposed a microfluidic model for thrombi formation in lung micro-vessel alveolar epithelial cells and the second with human vascular endothelial cells. The vascular channels enabled continuous whole-blood perfusion without the formation of thrombi under standard conditions. The reported system allows the quantification of dynamic platelet endothelial interactions followed by clot formation, which further demonstrates the role of the epithelium in inflammation-derived vascular thrombosis. The model mimics platelet–endothelial dynamics by including lipopolysaccharide (LPS) endotoxin to stimulate intravascular thrombosis. A protease-activated receptor-1 (PAR-1) antagonist was also applied to

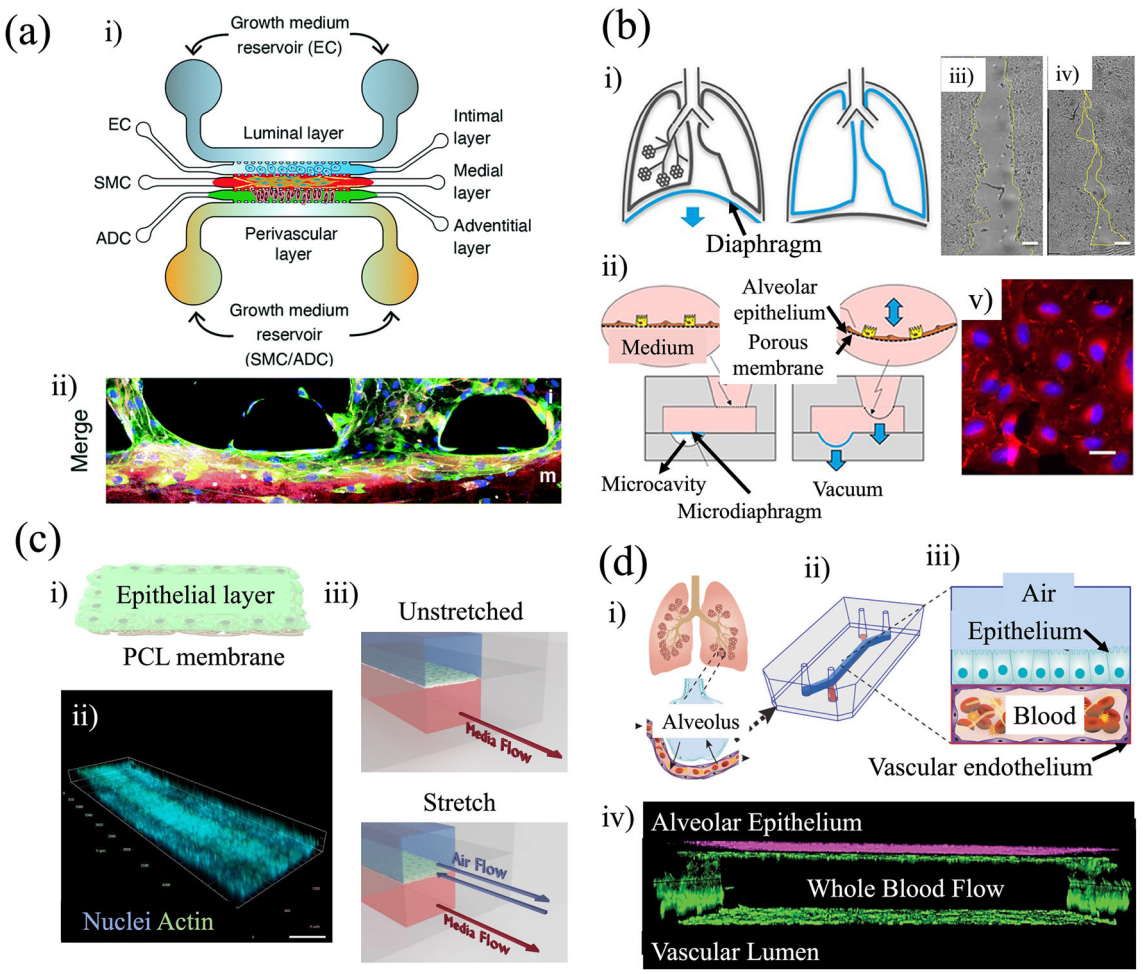

Fig. 5 Mimicking of lung pathologies. **a** Pulmonary hypertension-on-a-chip. (i) Multichannel microfluidic device mimicking the adventitial, medial, and intimal layers for growing adventitial cells (ADCs), smooth muscle cells (SMCs), and endothelial cells (ECs), respectively; (ii) a confocal 3D rendered image showing the distribution of PAH-ECs (pulmonary arterial hypertension—endothelial cells) and PAH-SMCs (pulmonary arterial hypertension—smooth muscle cells) in their matrix (scale bar: 75 μm). Reproduced from [51], Copyright 2020, with permission from The Royal Society of Chemistry. **b** Wound healing of alveolar lung epithelium in a microfluidic device. (i) Breathing concept in vivo. (ii) Breathing concept in vitro. A micro-diaphragm deflects in a defined microcavity. Due to the negative pressure generated, the alveolar membrane, where the cells are cultured, deflects downward. (iii) Lung cells immediately after wounding. (iv) Cells 24 h later. (v) Immunofluorescence image of A549 cells cultured on the membrane; nuclei are stained in blue, and ZO-1 in red (scale bar: 20 μm). Reproduced from [106], Copyright 2019, with permission from Frontiers, creative commons license (CC BY-NC-ND 4.0). **c** Modeling ventilator-induced lung injury. (i) Schematic illustration of MLE-12 alveolar epithelial cells; (ii) confocal fluorescence microscopy images of a MLE-12 layer (scale bar: 5 μm). (iii) Representation of the microfluidic device. Membrane stretch was achieved by blocking the outlet of the air channel and flowing air (108 mL/h) at a frequency of 0.1 Hz for 2 h (stretched condition). Reproduced from [104], Copyright 2021, with permission from the authors. **d** Lung thrombosis model. (i) Schematic of alveolar interaction with blood vessels; (ii) engineering drawing of the microfluidic device; (iii) illustration of human primary alveolar epithelial cells and human endothelial cells forming a lumen; (iv) side view of confocal micrographs showing junctional structures, the primary alveolar epithelium (purple, E-cadherin), and endothelium (green, VE-cadherin), through which blood perfusion takes place (scale bar: 100 μm). Reproduced from [105], Copyright 2017, with permission from American Society for Clinical Pharmacology and Therapeutics

demonstrate its usability as an antithrombotic therapeutic agent (Fig. 5d).

Drug screening

Microfluidic systems integrated with tissue engineering have recently been established as effective engineering tools with the ability to mimic complex human microphysiological environments and thus facilitate toxicology and drug-screening studies [110]. For example, Zhang et al. [71] proposed the use of a lung-on-a-chip to evaluate pulmonary cytotoxicity assays after treatment with nanoparticles. A co-culture of human pulmonary alveolar epithelial cells and human endothelial umbilical cells was carried out to expose endothelial cells to blood circulation by establishing medium

flow. To mimic acute pulmonary nanoparticle exposure, zinc oxide (ZnO) and titanium oxide (TiO_2) nanoparticles were administered to the epithelial cells. The model offered the capability to study the alteration of alveolar barrier integrity, barrier permeability, and protein expression with different nanoparticle concentrations. Another group, Mani et al. [111], presented a bioengineered lung cancer model with controlled fluid flow and pressure difference, for studying the interplay between physical and mechanical forces in cancer initiation, progression, and response to drug treatment. They reported a study on the contribution of flow-induced shear stress to the epithelial-to-mesenchymal transition (EMT) and also assessed the response of 3D cancer tumoroids to treatment with erlotinib and NSC-750212 (an experimental drug). The model demonstrates the capacity of shear stress to induce EMT in lung tumoroids. Interestingly, a distinct response to drug treatment of the tumoroids was observed under dynamic and static conditions. This phenomenon also distinctly indicates the advantage of the perfusion culture model over conventional static cultures for a better understanding of the in vivo counterpart process.

Another group, Meghani et al. [112], fabricated a lung-on-a-chip model with integrated sensors to evaluate epithelium electrical resistance and to apply pH-responsive ZnO quantum dots (QDs) encapsulated in human serum albumin (HSA) nanoparticles as a possible therapy. The model closely mimics cancerous alveolar epithelium by embedding lung cancer cells, stromal cells, and fibroblasts in a collagen matrix. The non-toxic ZnO quantum dots resulted in internalization inside the cancer cells due to the enhanced permeability and retention effect. The proposed in vitro model allowed real-time assessment of cytotoxicity and cellular uptake of HSA-ZnO for lung cancer cells, so it could be applied for nano-particle conjugated drug treatments.

Cancer therapeutics

Chemotherapy is the extensively reported primary treatment strategy for lung cancer; however, it faces multiple challenges due to the drug resistance ability of the cancer cells. This phenomenon led to the need for the development of reliable, cost-effective, and high-throughput engineered systems to test drug sensitivity and optimization of drug doses. To address this, Xu et al. [113] proposed a microfluidic co-cultured platform of stroma and patient-derived lung cancer cells. The model was tested for different anticancer drugs (i.e., gefitinib, paclitaxel, and gemcitabine) by introducing a concentration gradient generated within the microfluidic device. The device uses diffusive mixing to create a drug-concentration ratio of 5:6:8. The sensitivity of single and combined drug schemes was investigated while reconstructing the tumor microenvironment in vitro with continuous nutrient supplementation. The group successfully screened single or combined anti-cancer drug schemes for actual patient-derived cells in an efficient and accurate way.

Another group, Yang et al. [114], used electrospun poly(lactic-co-glycolic acid) (PLGA), a porous membrane which was found to play an essential role in biomimicry of the in vitro lung model, to construct a lung cancer-on-a-chip platform. The electrospun membrane had a thickness of about 3 μm, sufficient porosity, and the desired permeability for the biologically active molecules. In this model, A549 cells were co-cultured with human fetal lung fibroblasts (HLF1), along with HUVECs. The group characterized the nanofiber diameter, the permeability of the PLGA membrane, and its ability to provide a suitable substrate for lung cell attachment and growth. In addition, gefitinib, an anti-tumor drug that targets epidermal growth factor receptors (EGFRs) for metastatic lung cancer, was administered, and its effect on A549 cells was evaluated by applying fluorescent microscopy of E-Cad and EGFR. Finally, the destruction of endothelium by migration of lung cancer cells was confirmed by time-lapse images and the disruption of the platelet endothelial cell adhesion molecule CD31.

Antiviral drugs

The need for clinically accurate lung models became more evident during the recent pandemic caused by the novel coronavirus *n*CoV-19, also known as a severe acute respiratory syndrome coronavirus-2 (SARS-CoV-2) outbreak [115, 116]. It has been assumed that the acute immune response and generation of cell debris resulting from SARS-CoV-2 infection cause lung injury upon COVID-19 infection [117–119]. However, the mechanism of lung infection needs to be better understood so that efforts can be made to minimize lung fibrosis, which is identified as the prime cause of morbidity, even after clearance of SARS-CoV-2 by the immune system. Recently, Zhang et al. [120] recapitulated the alveolar–capillary barrier by co-culture of the alveolar epithelium, microvascular endothelium, and circulating immune cells. Activation of the epithelial innate immune response by cytokine-dependent pathways was observed after three days of infection. It was also evident that the viral infection caused endothelial detachment in the proposed system. The on-chip model was also examined for treatment with remdesivir, which is reported to reduce the severity of viral infection for patients infected with SARS-CoV-2 (Fig. 6a). Si et al. [121] also presented a micro-physiological system with a pseudo-typed infection of SARS-CoV-2. They administered amodiaquine, an anti-malarial drug that can inhibit the infection; however, clinical doses of hydroxychloroquine were unable to prevent the entry of pseudo-typed SARS-CoV-2 in cell lines. Another group, Huang et al. [53] reported a SARS-CoV-2 pseudo-viral infection in an alveolar lung-on-a-chip model, which

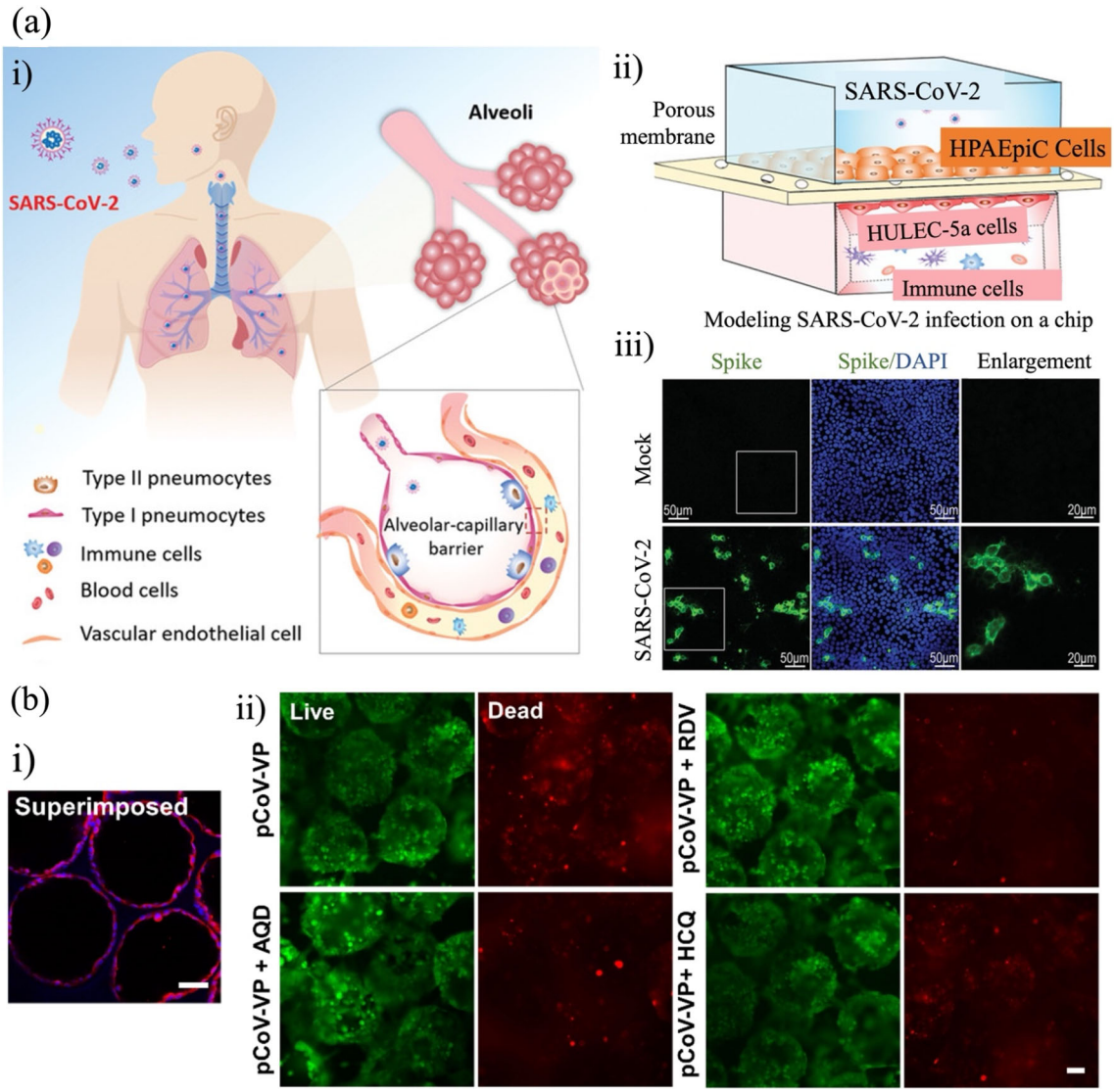

Fig. 6 Lung-on-a-chip and COVID-19. **a** Biomimetic model of SARS-CoV-2-induced lung injury. (i) Illustration of human alveolus barrier in vivo; (ii) configuration of human alveolus chip infected by SARS-CoV-2: (iii) Immunofluorescence micrographs showing viral Spike protein (Spike protein S1 subunit of SARS-CoV-2) staining in human pulmonary alveolar epithelial cells (HPAEpiCs) on day 3 post-infection. Reproduced from [120], Copyright 2020, with permission from the authors. **b** SARS-CoV-2 pseudo-viral infection and treatment efficacies in the alveolar lung-on-a-chip model; (i) fluorescence image showing the expression of ACE2 receptors by human alveolar epithelial cells (hAECs) (red, ACE2 receptors; blue, nuclei); (ii) fluorescence microscopic images showing the live/dead staining hAECs in the gelatin methacryloyl (GelMA) inverse opal structures after pCoV-VP+AQD, i.e., alveoli model infected with SARS-CoV-2 pseudoviral particles and treated with 5-μmol/L amodiaquine. Reproduced from [53], Copyright 2021, with permission from PNAS, creative commons license (CC BY-NC-ND 4.0)

involved applying SARS-CoV-2 pseudo-viral particles to study treatment efficacies of amodiaquine, remdesivir, and hydroxychloroquine, which are clinically approved antiviral drugs. They showed that the cytopathic effects of pseudo-viral particles were reduced upon administration of these drugs, thus preventing infection-induced death of alveolar cells after pseudo-viral infection (Fig. 6b). These lung-on-a-chip models can closely imitate human physiological responses to SARS-CoV-2 infection, thus serving as a unique platform for COVID-19 research and exploration of possible drugs.

Another group, Si et al. [121], investigated a novel microfluidic bronchial-airway-on-a-chip composed of human bronchial-airway epithelium and pulmonary endothelium. The model was studied for viral infection, strain-dependent virulence, cytokine production, and circulating immune cell activation. Further, influenza A infection was produced in the microphysiological system

to test the effectiveness of nafamostat, an anticoagulant drug, along with oseltamivir, which is a first-line antiviral drug. The model demonstrated a pharmacological strategy in which co-administration of these two drugs doubled the oseltamivir treatment time. Subsequently, the system was subjected to a pseudo-typed SARS-CoV-2 virus infection to evaluate the possible application of three well-known antimalarial drugs, i.e., chloroquine, hydroxychloroquine, and amodiaquine. The drugs were perfused to the infected systems at clinical concentrations. Chloroquine and hydroxychloroquine failed to inhibit the entry of the pseudo-virus, thus predicting failure. In contrast, amodiaquine showed a prophylactic effect against SARS-CoV-2 pseudo-virus. The results showed the capability of the proposed in vitro model to accelerate the identification of potential drugs to treat SARS-CoV-2 infection.

In vitro modeling of human lung functions

Morphology, breathing patterns, and physical forces are essential aspects of lung function, and are necessary to recapitulate for relevant replication when modeling the lung in vitro. Recently, a second-generation lung-on-a-chip model was established that goes further than the application of porous membranes in parallel channels with a 2D-like cell microenvironment. It could actually be considered a real 3D architecture of human lung alveoli. Stucki et al. [50] mimicked the pulmonary parenchymal environment and the cyclic strain of breathing movements. To achieve this, they assembled a PDMS membrane onto a pneumatic part which stretched the alveolar-like barrier to enable 3D cyclic strain in all directions (Fig. 7a). The minimal functional unit of the lungs is the alveolus, which is responsible for gas exchange with the atmosphere. Many approaches have been proposed to recapitulate the anatomy and physiology of the alveoli. For instance, Long et al. [122] proposed an optimized microfabricated lung-on-a-chip model that operated under continuous or periodic flow patterns of the culture medium. However, this optimization was performed without the use of cells.

Another group, Huang et al. [53], recently presented a model of the human pulmonary alveoli, composed of 3D porous hydrogel shaped in an inverse opal fashion, emulating human alveolar sacs (Fig. 7b). By seeding primary human alveolar epithelial cells, they achieved functional epithelial monolayers. Cycling contractions were applied to mimic breathing events, thus enabling a new platform for studying pathological effects of cigarettes, viral infection, or contamination. Zamprogno et al. [51] also proposed a stretchable alveolar model that reproduced alveolar distribution. It had dimensions similar to those found in vivo, which they achieved by culturing cells on stretchable lung ECM proteins (Fig. 7c). The biological membrane was drop-casted onto a honeycomb gold mesh to support the array of 40 alveoli. Primary epithelial and endothelial human lung cells were co-cultured over the membrane and exposed to stretching forces. This model achieved lung alveolar arrays that were able to display parenchymal characteristics [51]. Another group, Schimek et al. [68], investigated homeostasis in a microphysiological system composed of two organ models that incorporated lung cells in a reservoir; the system was provided with an air-permeable membrane and liver spheroids to allow testing of the cytotoxicity of inhaled substances (Fig. 7d). It was treated with a hepatotoxic and carcinogenic aflatoxin B1 which resulted in impaired functionality in lung tissues.

Commercially developed lung-on-a-chip devices

The milestones achieved so far in the area of lung-on-a-chip devices are becoming more prominent with the development of new startups working solely on the application of these microfluidic devices to analyze the pathophysiological aspects of human lungs. One such promising startup is Emulate. Inc., created by Donald E. Ingber at the Labs of Wyss Institute for Biologically Inspired Engineering, at Harvard. They offer two different lung-on-a-chip models: the Alveolus Lung-Chip [105] and the Airway Lung-Chip [93]. Both models have proven ability in drug efficacy studies and for analyzing pathophysiological behavior of primary human lung cells under different disease conditions. Another notable company working on modeling lung pathophysiology in a microfluidic chip is AlveoliX AG, based in Switzerland. They fabricate lungs-on-a-chip by mimicking the lung biophysical microenvironment, which they generate by including thin, porous membranes with controlled mechanical motion, placed on the lung alveoli to create physiologically relevant breathing conditions. This technology offers dynamic breathing, which improves the relevance of the model with the in vivo event cascades that occur under normal and disease conditions [123].

Conclusions and perspective

Several lung-on-a-chip models have been designed and their efficacy has been proved for studying lung disease and analyzing the potential effects of drugs. Compared to traditional 2D models and 3D-static culture models, they have exclusive abilities to maintain functional human lung cells with better physicochemical characteristics. However, drawbacks still exist and need to be analyzed for further improvement. For example, most lung-on-a-chip models include immortalized and adenocarcinoma cell lines, which impart deviated functionality compared to primary human lung cells [124]. This may lead to inaccurate assessment of functional response to

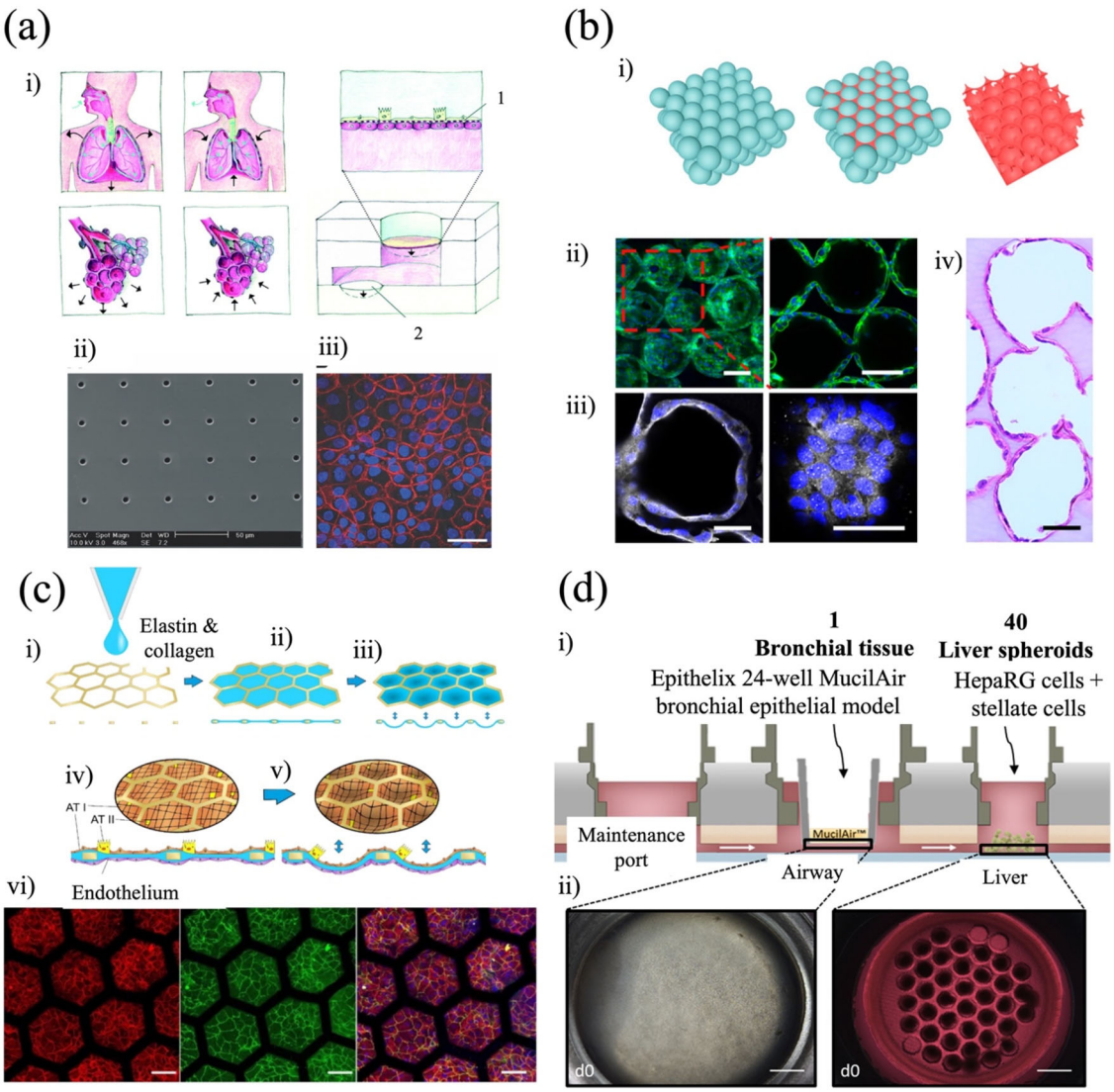

Fig. 7 In vitro modeling of human lung functions. **a** Lung-on-a-chip with respiration mechanism. (i) In vivo respiration is controlled by the diaphragm, whose contraction leads to 3D expansion of the alveolar sacs; in vitro, the 3D cyclic mechanical strain of the bioartificial alveolar membrane (1) induced by a micro-diaphragm (2) actuated by an electro-pneumatic setup. (ii) Porous and flexible polydimethylsiloxane (PDMS) membrane used as a cell-culture substrate; (iii) Z-projection of a confluent layer of lung epithelial cells (16HBE14o−) stained for adherens-junction E-cadherin (red) and cell nuclei (blue) (scale bars: 50 μm). Reproduced from [50], Copyright 2015, with permission from The Royal Society of Chemistry. **b** Inverse-opal lung-on-a-chip model. (i) Fabrication of the model; (ii) fluorescence image of human alveolar epithelial cells (hAECs) after culturing inverse-opal hydrogel structure (green, F-actin; blue, nuclei; scale bars: 100 μm); (iii) micrographs showing the presence of continuous tight junctions of the rim (white, ZO-1; blue, nuclei; scale bars: 50 μm). (iv) H&E-stained section of the alveolar lung model (scale bar: 100 μm). Reproduced from [53], Copyright 2021, with permission from the authors. **c** Representation of the stretchable alveolar model. Thin honeycomb gold mesh (diameter 260 μm) was used as a scaffold to drop collagen–elastin solution for cell culture; human alveolar type I-like cells (hAEpC) were cultured on the hexagonal mesh with the collagen–elastin membrane after 4 days and at the air–liquid interface for 2 days. Expression of adherens-junction markers (E-cadherin, red), tight junctions with zonula occludens-1 (ZO-1, green), and merged (Hoechst, blue; E-cadherin, red; ZO-1, green). Scale bar: 100 μm. Reproduced from [51], Copyright 2021, with permission from the authors. **d** Human multiorgan-on-a-chip. (i) The multi-organ chip platform and experimental setup; (ii) forty liver spheroids and one bronchial MucilAir culture were placed in the device (scale bar: 1000 μm). Reproduced from [68], Copyright 2020, with permission from the authors

an external stimulus. Also, in microfluidic devices the volume of media flow often exceeds the volume of the embedded tissue, which causes dilution of secreted metabolites and biologically active molecules [44]. This phenomenon can negatively affect cell-signaling pathways, specifically when applied in a single-pass perfusion device. The surface-to-volume ratio is another parameter to consider when studying the effect of autocrine and paracrine cell-signaling pathways, which may differ when the concentration of signaling molecules secreted by cells is reduced [125]. Another major issue reported so far is the use of PDMS as a material in fabricating microfluidic devices. Because of the ability of PDMS to adsorb small hydrophobic molecules, there may be considerable alteration to concentrations of cell-secreted molecules or added drugs [126]. To overcome this major challenge, other materials such as poly(itaconate-co-citrate-co-octanediol), poly(octamethylene maleate (anhydride) citrate) (POMaC) polymer, tetrafluoroethylene propylene (FEPM), poly(polyol sebacate), and poly(ester amide) elastomers have been successfully evaluated and found to be good alternatives to PDMS. Another much-discussed thermoplastic elastomer styrene–ethylene–butylene–styrene (SEBS) showed 10% and 21% lower absorption of pirfenidone and rhodamine B (two model drug molecules), respectively, when compared to a device made with PDMS. Aside from elastomers, many thermoplastics, e.g., poly(lactic acid) (PLA), polyethylene terephthalate (PET), and poly(methyl methacrylate) (PMMA), are drawing considerable research interest for their potential to overcome the shortcomings of PDMS in the field of microfabrication and organ-on-a-chip construction [127].

Furthermore, the introduction of immune components which play crucial roles in disease progression and the healing process can improve in vivo relevance [128]. Considering and addressing these factors would allow establishment of a superior microfluidic model for in vitro modeling of lung disease. Such models can also convincingly address the ethical and regulatory concerns of using animal models for preclinical applications. Advancements in this field require the collaboration of experts from multidisciplinary sectors to fabricate an effective device for high-throughput screening of potential drugs to cure respiratory diseases.

Acknowledgements We gratefully thank the startup funding of R.E. by the Henry Samueli School of Engineering and the Department of Electrical Engineering at the University of California, Irvine. J.A.T-N. acknowledges the Consejo Nacional de Ciencia y Tecnología (CONACyT, Mexico) and the University of California for the support provided under the UC MEXUS-CONACYT doctoral fellowships.

Author contributions RE conceptualized the paper. JATN, PD, SN, and RE collected the data and wrote the original draft. JATN, PD, SN, SZ, and RE reviewed and edited the document. All authors provided feedback.

Declarations

Conflict of interest The authors declare that they have no conflict of interest.

Ethical approval This article does not contain any studies with human or animal subjects performed by any of the authors.

References

1. Levine SM, Marciniuk DD (2022) Global impact of respiratory diseases: what can we do, together, to make a difference? Chest 161(5):1153–1154. https://doi.org/10.1016/j.chest.2022.01.014
2. Cotes JE, Chinn DJ, Miller MR (2006) Lung Function: Physiology, Measurement and Application in Medicine (6th Ed.). Blackwell Pub, Malden
3. Sung H, Ferlay J, Siegel RL et al (2021) Global cancer statistics 2020: GLOBOCAN estimates of incidence and mortality worldwide for 36 cancers in 185 countries. CA Cancer J Clin 71(3):209–249. https://doi.org/10.3322/caac.21660
4. Artzy-Schnirman A, Hobi N, Schneider-Daum N et al (2019) Advanced in vitro lung-on-chip platforms for inhalation assays: from prospect to pipeline. Eur J Pharm Biopharm 144:11–17. https://doi.org/10.1016/j.ejpb.2019.09.006
5. Cron RQ, Caricchio R, Chatham WW (2021) Calming the cytokine storm in COVID-19. Nat Med 27(10):1674–1675. https://doi.org/10.1038/s41591-021-01500-9
6. Ho JQ, Sepand MR, Bigdelou B et al (2022) The immune response to COVID-19: does sex matter? Immunology 166(4):429–443. https://doi.org/10.1111/imm.13487
7. Van Norman GA (2019) Limitations of animal studies for predicting toxicity in clinical trials: is it time to rethink our current approach? JACC Basic Transl Sci 4(7):845–854. https://doi.org/10.1016/j.jacbts.2019.10.008
8. Bhowmick R, Derakhshan T, Liang Y et al (2018) A three-dimensional human tissue-engineered lung model to study influenza A infection. Tissue Eng Part A 24(19–20):1468–1480. https://doi.org/10.1089/ten.TEA.2017.0449
9. Mazrouei R, Velasco V, Esfandyarpour R (2020) 3D-bioprinted all-inclusive bioanalytical platforms for cell studies. Sci Rep 10:14669. https://doi.org/10.1038/s41598-020-71452-6
10. Velasco V, Shariati SA, Esfandyarpour R (2020) Microtechnology-based methods for organoid models. Microsyst Nanoeng 6:76. https://doi.org/10.1038/s41378-020-00185-3
11. Shrestha J, Razavi Bazaz S, Aboulkheyr Es H et al (2020) Lung-on-a-chip: the future of respiratory disease models and pharmacological studies. Crit Rev Biotechnol 40(2):213–230. https://doi.org/10.1080/07388551.2019.1710458
12. Birgersdotter A, Sandberg R, Ernberg I (2005) Gene expression perturbation in vitro—a growing case for three-dimensional (3D) culture systems. Semin Cancer Biol 15(5):405–412. https://doi.org/10.1016/j.semcancer.2005.06.009
13. Velasco V, Joshi K, Chen J et al (2019) Personalized drug efficacy monitoring chip. Anal Chem 91(23):14927–14935. https://doi.org/10.1021/acs.analchem.9b03291
14. Esfandyarpour R, Esfandyarpour H, Harris JS et al (2013) Simulation and fabrication of a new novel 3D injectable biosensor for high throughput genomics and proteomics in a lab-on-a-chip device. Nanotechnology 24(46):465301. https://doi.org/10.1088/0957-4484/24/46/465301
15. Esfandyarpour R, Esfandyarpour H, Javanmard M et al (2012) Electrical detection of protein biomarkers using nanoneedle

biosensors. MRS Online Proc Libr 1414(1):7–14. https://doi.org/10.1557/opl.2012.807
16. Esfandyarpour R, Esfandyarpour H, Javanmard M et al (2013) Microneedle biosensor: a method for direct label-free real time protein detection. Sens Actuat B Chem 177:848–855. https://doi.org/10.1016/j.snb.2012.11.064
17. Esfandyarpour R, Javanmard M, Harris J et al (2014) Label-free electronic detection of target cells. Proc SPIE 1:8976. https://doi.org/10.1117/12.2037966
18. Kumar S, Esfandyarpour R, Davis R et al (2014) Surface charge sensing by altering the phase transition in VO2. J Appl Phys 116(7):074511. https://doi.org/10.1063/1.4893577
19. Esfandyarpour R, DiDonato MJ, Yang Y et al (2017) Multifunctional, inexpensive, and reusable nanoparticle-printed biochip for cell manipulation and diagnosis. Proc Natl Acad Sci USA 114(8):E1306–E1315. https://doi.org/10.1073/pnas.1621318114
20. Esfandyarpour R, Koochak Z, Harris JS et al (2015) Rapid, label free, high throughput, miniaturized, and inexpensive nanoelectronic array as a cancer diagnosis tool. In: 18th International Conference on Solid-State Sensors, Actuators and Microsystems (Transducers), pp. 1523–1526
21. Esfandyarpour R, Yang L, Koochak Z et al (2016) Nanoelectronic three-dimensional (3D) nanotip sensing array for real-time, sensitive, label-free sequence specific detection of nucleic acids. Biomed Microdevices 18(1):7. https://doi.org/10.1007/s10544-016-0032-8
22. Joshi K, Esfandyarpour R (2020) An inkjet-printed and reusable platform for single cell impedance cytometry. Microfluidics Biomems Med Microsyst 18:11235. https://doi.org/10.1117/12.2543160
23. Joshi K, Javani A, Park J et al (2020) A machine learning-assisted nanoparticle-printed biochip for real-time single cancer cell analysis. Adv Biosyst 4(11):2000160. https://doi.org/10.1002/adbi.202000160
24. Joshi K, Velasco V, Esfandyarpour R (2020) A low-cost, disposable and portable inkjet-printed biochip for the developing world. Sensors 20(12):3593. https://doi.org/10.3390/s20123593
25. Elbert KJ, Schafer UF, Schafers HJ et al (1999) Monolayers of human alveolar epithelial cells in primary culture for pulmonary absorption and transport studies. Pharm Res 16(5):601–608. https://doi.org/10.1023/a:1018887501927
26. Sucre JMS, Jetter CS, Loomans H et al (2018) Successful establishment of primary type II alveolar epithelium with 3D organotypic coculture. Am J Respir Cell Mol Biol 59(2):158–166. https://doi.org/10.1165/rcmb.2017-0442MA
27. Evans KV, Lee JH (2020) Alveolar wars: the rise of in vitro models to understand human lung alveolar maintenance, regeneration, and disease. Stem Cells Transl Med 9(8):867–881. https://doi.org/10.1002/sctm.19-0433
28. Jiang D, Schaefer N, Chu HW (2018) Air–liquid interface culture of human and mouse airway epithelial cells. Methods Mol Biol 1809:91–109. https://doi.org/10.1007/978-1-4939-8570-8_8
29. Bluhmki T, Bitzer S, Gindele JA et al (2020) Development of a miniaturized 96-transwell air-liquid interface human small airway epithelial model. Sci Rep 10:13022. https://doi.org/10.1038/s41598-020-69948-2
30. Xu W, Janocha AJ, Leahy RA et al (2014) A novel method for pulmonary research: assessment of bioenergetic function at the air–liquid interface. Redox Biol 2:513–519. https://doi.org/10.1016/j.redox.2014.01.004
31. Fang Y, Eglen RM (2017) Three-dimensional cell cultures in drug discovery and development. SLAS Discov 22(5):456–472. https://doi.org/10.1177/1087057117696795
32. Hofer M, Lutolf MP (2021) Engineering organoids. Nat Rev Mater 6(5):402–420. https://doi.org/10.1038/s41578-021-00279-y
33. Kim J, Koo BK, Knoblich JA (2020) Human organoids: model systems for human biology and medicine. Nat Rev Mol Cell Biol 21(10):571–584. https://doi.org/10.1038/s41580-020-0259-3
34. Cores J, Dinh PC, Hensley T et al (2020) A pre-investigational new drug study of lung spheroid cell therapy for treating pulmonary fibrosis. Stem Cells Transl Med 9(7):786–798. https://doi.org/10.1002/sctm.19-0167
35. Dinh PC, Cores J, Hensley MT et al (2017) Derivation of therapeutic lung spheroid cells from minimally invasive transbronchial pulmonary biopsies. Respir Res 18:132. https://doi.org/10.1186/s12931-017-0611-0
36. Li Z, Qian Y, Li W et al (2020) Human lung adenocarcinoma-derived organoid models for drug screening. iScience 23(8):1011. https://doi.org/10.1016/j.isci.2020.101411
37. Mehta G, Hsiao AY, Ingram M et al (2012) Opportunities and challenges for use of tumor spheroids as models to test drug delivery and efficacy. J Contr Release 164(2):192–204. https://doi.org/10.1016/j.jconrel.2012.04.045
38. Crabbé A, Liu Y, Sarker SF et al (2015) Recellularization of decellularized lung scaffolds is enhanced by dynamic suspension culture. PLoS ONE 10(5):e0126846. https://doi.org/10.1371/journal.pone.0126846
39. Allen AB, Priddy LB, Li MT et al (2015) Functional augmentation of naturally-derived materials for tissue regeneration. Ann Biomed Eng 43(3):555–567. https://doi.org/10.1007/s10439-014-1192-4
40. Rezaei FS, Khorshidian A, Beram FM et al (2021) 3D printed chitosan/polycaprolactone scaffold for lung tissue engineering: hope to be useful for COVID-19 studies. RSC Adv 11(32):19508–19520. https://doi.org/10.1039/d1ra03410c
41. Wang X, Zhang X, Dai X et al (2018) Tumor-like lung cancer model based on 3D bioprinting. 3 Biotech 8(12):501. https://doi.org/10.1007/s13205-018-1519-1
42. Young BM, Shankar K, Allen BP et al (2017) Electrospun decellularized lung matrix scaffold for airway smooth muscle culture. ACS Biomater Sci Eng 3(12):3480–3492. https://doi.org/10.1021/acsbiomaterials.7b00384
43. Wan X, Ball S, Willenbrock F et al (2017) Perfused three-dimensional organotypic culture of human cancer cells for therapeutic evaluation. Sci Rep 7:9408. https://doi.org/10.1038/s41598-017-09686-0
44. Halldorsson S, Lucumi E, Gomez-Sjoberg R et al (2015) Advantages and challenges of microfluidic cell culture in polydimethylsiloxane devices. Biosens Bioelectron 63:218–231. https://doi.org/10.1016/j.bios.2014.07.029
45. Kim T, Yi Q, Hoang E et al (2021) A 3D printed wearable bioelectronic patch for multi-sensing and in situ sweat electrolyte monitoring. Adv Mater Technol 6(4):2001021. https://doi.org/10.1002/admt.202001021
46. Ruzycka M, Cimpan MR, Rios-Mondragon I et al (2019) Microfluidics for studying metastatic patterns of lung cancer. J Nanobiotechnol 17:71. https://doi.org/10.1186/s12951-019-0492-0
47. Zhang M, Xu C, Jiang L et al (2018) A 3D human lung-on-a-chip model for nanotoxicity testing. Toxicol Res 7(6):1048–1060. https://doi.org/10.1039/c8tx00156a
48. Huh D, Matthews BD, Mammoto A et al (2010) Reconstituting organ-level lung functions on a chip. Science 328(5986):1662–1668. https://doi.org/10.1126/science.1188302
49. Huh DD (2015) A human breathing lung-on-a-chip. Ann Am Thorac Soc 12(Suppl 1):S42–S44. https://doi.org/10.1513/AnnalsATS.201410-442MG
50. Stucki AO, Stucki JD, Hall SR et al (2015) A lung-on-a-chip array with an integrated bio-inspired respiration mechanism. Lab Chip 15(5):1302–1310. https://doi.org/10.1039/c4lc01252f

51. Zamprogno P, Wuthrich S, Achenbach S et al (2021) Second-generation lung-on-a-chip with an array of stretchable alveoli made with a biological membrane. Commun Biol 4:168. https://doi.org/10.1038/s42003-021-01695-0
52. Ochs M, Nyengaard JR, Jung A et al (2004) The number of alveoli in the human lung. Am J Respir Crit Care Med 169(1):120–124. https://doi.org/10.1164/rccm.200308-1107OC
53. Huang D, Liu T, Liao J et al (2021) Reversed-engineered human alveolar lung-on-a-chip model. Proc Natl Acad Sci USA 118(19):e2016146118. https://doi.org/10.1073/pnas.2016146118
54. Aleman J, Kilic T, Mille LS et al (2021) Microfluidic integration of regeneratable electrochemical affinity-based biosensors for continual monitoring of organ-on-a-chip devices. Nat Protoc 16(5):2564–2593. https://doi.org/10.1038/s41596-021-00511-7
55. Srinivasan B, Kolli AR, Esch MB et al (2015) TEER measurement techniques for in vitro barrier model systems. J Lab Autom 20(2):107–126. https://doi.org/10.1177/2211068214561025
56. Bovard D, Giralt A, Trivedi K et al (2020) Comparison of the basic morphology and function of 3D lung epithelial cultures derived from several donors. Curr Res Toxicol 1:56–69. https://doi.org/10.1016/j.crtox.2020.08.002
57. Henry OYF, Villenave R, Cronce MJ et al (2017) Organs-on-chips with integrated electrodes for trans-epithelial electrical resistance (TEER) measurements of human epithelial barrier function. Lab Chip 17(13):2264–2271. https://doi.org/10.1039/c7lc00155j
58. Molloy K, Cagney G, Dillon ET et al (2020) Impaired airway epithelial barrier integrity in response to stenotrophomonas maltophilia proteases, novel insights using cystic fibrosis bronchial epithelial cell secretomics. Front Immunol 11:198. https://doi.org/10.3389/fimmu.2020.00198
59. Doryab A, Taskin MB, Stahlhut P et al (2021) A bioinspired in vitro lung model to study particokinetics of nano-/microparticles under cyclic stretch and air-liquid interface conditions. Front Bioeng Biotechnol 9:616830. https://doi.org/10.3389/fbioe.2021.616830
60. Mermoud Y, Felder M, Stucki JD et al (2018) Microimpedance tomography system to monitor cell activity and membrane movements in a breathing lung-on-chip. Sensor Actuat B Chem 255:3647–3653. https://doi.org/10.1016/j.snb.2017.09.192
61. Skardal A, Murphy SV, Devarasetty M et al (2017) Multi-tissue interactions in an integrated three-tissue organ-on-a-chip platform. Sci Rep 7:8837. https://doi.org/10.1038/s41598-017-08879-x
62. Zhang F, Liu WM, Zhou SS et al (2020) Investigation of environmental pollutant-induced lung inflammation and injury in a 3D coculture-based microfluidic pulmonary alveolus system. Anal Chem 92(10):7200–7208. https://doi.org/10.1021/acs.analchem.0c00759
63. Mejías JC, Nelson MR, Liseth O et al (2020) A 96-well format microvascularized human lung-on-a-chip platform for microphysiological modeling of fibrotic diseases. Lab Chip 20(19):3601–3611. https://doi.org/10.1039/d0lc00644k
64. Lee SW, Kwak HS, Kang MH et al (2018) Fibroblast-associated tumour microenvironment induces vascular structure-networked tumouroid. Sci Rep 8:2365. https://doi.org/10.1038/s41598-018-20886-0
65. Das P, Najafikhoshnoo S, Tavares-Negrete JA et al (2022) An in-vivo-mimicking 3D lung cancer-on-a-chip model to study the effect of external stimulus on the progress and inhibition of cancer metastasis. Bioprinting 28:e00243 https://doi.org/10.1016/j.bprint.2022.e00243
66. Khalid MAU, Kim YS, Ali M et al (2020) A lung cancer-on-chip platform with integrated biosensors for physiological monitoring and toxicity assessment. Biochem Eng J 155:107469. https://doi.org/10.1016/j.bej.2019.107469
67. Al-Hilal TA, Keshavarz A, Kadry H et al (2020) Pulmonary-arterial-hypertension (PAH)-on-a-chip: fabrication, validation and application. Lab Chip 20(18):3334–3345. https://doi.org/10.1039/d0lc00605j
68. Schimek K, Frentzel S, Luettich K et al (2020) Human multi-organ chip co-culture of bronchial lung culture and liver spheroids for substance exposure studies. Sci Rep 10:7865. https://doi.org/10.1038/s41598-020-64219-6
69. Kim D, Chen Z, Zhou LF et al (2018) Air pollutants and early origins of respiratory diseases. Chronic Dis Transl Med 4(2):75–94. https://doi.org/10.1016/j.cdtm.2018.03.003
70. Reza Sepand M, Bigdelou B, Salek Maghsoudi A et al (2023) Ferroptosis: Environmental causes, biological redox signaling responses, cancer and other health consequences. Coord Chem Rev 480:215024. https://doi.org/10.1016/j.ccr.2023.215024
71. Zhang F, Tian C, Liu W et al (2018) Determination of benzopyrene-induced lung inflammatory and cytotoxic injury in a chemical gradient-integrated microfluidic bronchial epithelium system. ACS Sens 3(12):2716–2725. https://doi.org/10.1021/acssensors.8b01370
72. Xu C, Zhang M, Chen W et al (2020) Assessment of air pollutant PM2.5 pulmonary exposure using a 3D lung-on-chip model. ACS Biomater Sci Eng 6(5):3081–3090. https://doi.org/10.1021/acsbiomaterials.0c00221
73. Plebani R, Potla R, Soong M et al (2022) Modeling pulmonary cystic fibrosis in a human lung airway-on-a-chip. J Cyst Fibros 21(4):606–615. https://doi.org/10.1016/j.jcf.2021.10.004
74. Islami F, Goding Sauer A, Miller KD et al (2018) Proportion and number of cancer cases and deaths attributable to potentially modifiable risk factors in the United States. CA Cancer J Clin 68(1):31–54. https://doi.org/10.3322/caac.21440
75. Shrestha J, Ghadiri M, Shanmugavel M et al (2019) A rapidly prototyped lung-on-a-chip model using 3D-printed molds. Organs-on-a-Chip 1:100001. https://doi.org/10.1016/j.ooc.2020.100001
76. Jones B, Donovan C, Liu G et al (2017) Animal models of COPD: what do they tell us? Respirology 22(1):21–32. https://doi.org/10.1111/resp.12908
77. Hou W, Hu SY, Yong KT et al (2020) Cigarette smoke-induced malignant transformation via STAT3 signalling in pulmonary epithelial cells in a lung-on-a-chip model. Bio-Des Manuf 3(4):383–395. https://doi.org/10.1007/s42242-020-00092-6
78. Benam KH, Novak R, Ferrante TC et al (2020) Biomimetic smoking robot for in vitro inhalation exposure compatible with microfluidic organ chips. Nat Protoc 15(2):183–206. https://doi.org/10.1038/s41596-019-0230-y
79. Benam KH, Mazur M, Choe Y et al (2017) Human lung small airway-on-a-chip protocol. Methods Mol Biol 1612:345–365. https://doi.org/10.1007/978-1-4939-7021-6_25
80. Cetintas E, Luo Y, Nguyen C et al (2022) Characterization of exhaled e-cigarette aerosols in a vape shop using a field-portable holographic on-chip microscope. Sci Rep 12:3175. https://doi.org/10.1038/s41598-022-07150-2
81. Reyfman PA, Walter JM, Joshi N et al (2019) Single-cell transcriptomic analysis of human lung provides insights into the pathobiology of pulmonary fibrosis. Am J Respir Crit Care Med 199(12):1517–1536. https://doi.org/10.1164/rccm.201712-2410OC
82. Ratjen F, Bell SC, Rowe SM et al (2015) Cystic fibrosis. Nat Rev Dis Primers 1:15010. https://doi.org/10.1038/nrdp.2015.10
83. Park S, Kim TH, Kim SH et al (2021) Three-dimensional vascularized lung cancer-on-a-chip with lung extracellular matrix hydrogels for in vitro screening. Cancers 13(16):3930. https://doi.org/10.3390/cancers13163930

84. Xu Z, Li E, Guo Z et al (2016) Design and construction of a multi-organ microfluidic chip mimicking the in vivo microenvironment of lung cancer metastasis. ACS Appl Mater Interfaces 8(39):25840–25847. https://doi.org/10.1021/acsami.6b08746
85. Esfandyarpour R (2013) Electrical Response of DNA and Proteins at Nanoscale by Using Novel Nanoneedle Biosensor. Nanotech
86. Esfandyarpour R, Javanmard M, Koochak Z et al (2013) Thin film nanoelectronic probe for protein detection. MRS Online Proc Libr 1572:110. https://doi.org/10.1557/opl.2013.660
87. Esfandyarpour R, Javanmard M, Koochak Z et al (2013) Label-free electronic probing of nucleic acids and proteins at the nanoscale using the nanoneedle biosensor. Biomicrofluidics 1508 7(4):044114. https://doi.org/10.1063/1.4817771
88. Esfandyarpour R, Javanmard M, Koochak Z et al (2014) Matrix Independent Label-Free Nanoelectronic Biosensor. In: IEEE 27th International Conference on Micro Electro Mechanical Systems, pp. 1083–1086
89. Esfandyarpour R, Javanmard M, Koochak Z et al (2014) Nanoelectronic impedance detection of target cells. Biotechnol Bioeng 111(6):1161–1169. https://doi.org/10.1002/bit.25171
90. Esfandyarpour R, Kashi A, Nemat-Gorgani M et al (2019) A nanoelectronics-blood-based diagnostic biomarker for myalgic encephalomyelitis/chronic fatigue syndrome (ME/CFS). Proc Natl Acad Sci USA 116(21):10250–10257. https://doi.org/10.1073/pnas.1901274116
91. NajafiKhoshnoo S, Kim T, Tavares-Negrete JA et al (2023) A 3D nanomaterials-printed wearable, battery-free, biocompatible, flexible, and wireless pH sensor system for real-time health monitoring. Adv Mater Technol 8(8):2201655 https://doi.org/10.1002/admt.202201655
92. Yi Q, Najafikhoshnoo S, Das P et al (2022) All-3D-printed, flexible, and hybrid wearable bioelectronic tactile sensors using biocompatible nanocomposites for health monitoring. Adv Mater Technol 7(5):2101034. https://doi.org/10.1002/admt.202101034
93. Yi Q, Pei XC, Das P et al (2022) A self-powered triboelectric MXene-based 3D-printed wearable physiological biosignal sensing system for on-demand, wireless, and real-time health monitoring. Nano Energy 101:107511. https://doi.org/10.1016/j.nanoen.2022.107511
94. Pollet A, den Toonder JMJ (2020) Recapitulating the vasculature using organ-on-chip technology. Bioengineering 7(1):17. https://doi.org/10.3390/bioengineering7010017
95. Trujillo-de Santiago G, Flores-Garza BG, Tavares-Negrete JA et al (2019) The tumor-on-chip: recent advances in the development of microfluidic systems to recapitulate the physiology of solid tumors. Materials 12(18):2945. https://doi.org/10.3390/ma12182945
96. Dharmage SC, Perret JL, Custovic A (2019) Epidemiology of asthma in children and adults. Front Pediatr 7:246. https://doi.org/10.3389/fped.2019.00246
97. Pavord ID, Beasley R, Agusti A et al (2018) After asthma: redefining airways diseases. Lancet 391(10118):350–400. https://doi.org/10.1016/S0140-6736(17)30879-6
98. Abrams EM, Jong GW, Yang CL (2020) Asthma and COVID-19. CMAJ 192(20):E551. https://doi.org/10.1503/cmaj.200617
99. Nawroth JC, Lucchesi C, Cheng D et al (2020) A Microengineered airway lung chip models key features of viral-induced exacerbation of asthma. Am J Respir Cell Mol Biol 63(5):591–600. https://doi.org/10.1165/rcmb.2020-0010MA
100. Fan EKY, Fan J (2018) Regulation of alveolar macrophage death in acute lung inflammation. Respir Res 19:50. https://doi.org/10.1186/s12931-018-0756-5
101. Benam KH, Villenave R, Lucchesi C et al (2016) Small airway-on-a-chip enables analysis of human lung inflammation and drug responses in vitro. Nat Methods 13(2):151–157. https://doi.org/10.1038/nmeth.3697
102. Punde TH, Wu WH, Lien PC et al (2015) A biologically inspired lung-on-a-chip device for the study of protein-induced lung inflammation. Integr Biol 7(2):162–169. https://doi.org/10.1039/c4ib00239c
103. Chin KM, Rubin LJ (2008) Pulmonary arterial hypertension. J Am Coll Cardiol 51(16):1527–1538. https://doi.org/10.1016/j.jacc.2008.01.024
104. Tas S, Rehnberg E, Bölükbas DA et al (2021) 3D printed lung on a chip device with a stretchable nanofibrous membrane for modeling ventilator induced lung injury. bioRxiv:2021.2007.2002.450873 https://doi.org/10.1101/2021.07.02.450873
105. Jain A, Barrile R, van der Meer AD et al (2018) Primary human lung alveolus-on-a-chip model of intravascular thrombosis for assessment of therapeutics. Clin Pharmacol Ther 103(2):332–340. https://doi.org/10.1002/cpt.742
106. Felder M, Trueeb B, Stucki AO et al (2019) Impaired wound healing of alveolar lung epithelial cells in a breathing lung-on-a-chip. Front Bioeng Biotechnol 7:3. https://doi.org/10.3389/fbioe.2019.00003
107. Pinhu L, Whitehead T, Evans T et al (2003) Ventilator-associated lung injury. Lancet 361(9354):332–340. https://doi.org/10.1016/S0140-6736(03)12329-X
108. Rehnberg E, Tas S, Bölükbas DA et al (2021) Lung-on-a-chip device for modelling of ventilator induced lung injury. ERJ Open Research 7:1
109. Amoretti M, Amsler C, Bonomi G et al (2002) Production and detection of cold antihydrogen atoms. Nature 419(6906):456–459. https://doi.org/10.1038/nature01096
110. Vanegas MI, Hubbard KR, Esfandyarpour R et al (2019) Microinjectrode system for combined drug infusion and electrophysiology. Jove J Vis Exp 2019(153):e60365. https://doi.org/10.3791/60365
111. Mani V, Lyu Z, Kumar V et al (2019) Epithelial-to-mesenchymal transition (EMT) and drug response in dynamic bioengineered lung cancer microenvironment. Adv Biosyst 3(1):e1800223 https://doi.org/10.1002/adbi.201800223
112. Meghani N, Kim KH, Kim SH et al (2020) Evaluation and live monitoring of pH-responsive HSA-ZnO nanoparticles using a lung-on-a-chip model. Arch Pharm Res 43(5):503–513. https://doi.org/10.1007/s12272-020-01236-z
113. Xu Z, Gao Y, Hao Y et al (2013) Application of a microfluidic chip-based 3D co-culture to test drug sensitivity for individualized treatment of lung cancer. Biomaterials 34(16):4109–4117. https://doi.org/10.1016/j.biomaterials.2013.02.045
114. Yang X, Li K, Zhang X et al (2018) Nanofiber membrane supported lung-on-a-chip microdevice for anti-cancer drug testing. Lab Chip 18(3):486–495. https://doi.org/10.1039/c7lc01224a
115. George PM, Wells AU, Jenkins RG (2020) Pulmonary fibrosis and COVID-19: the potential role for antifibrotic therapy. Lancet Respir Med 8(8):807–815. https://doi.org/10.1016/S2213-2600(20)30225-3
116. Ojo AS, Balogun SA, Williams OT et al (2020) Pulmonary fibrosis in COVID-19 survivors: predictive factors and risk reduction strategies. Pulm Med 2020:6175964. https://doi.org/10.1155/2020/6175964
117. Mason RJ (2020) Pathogenesis of COVID-19 from a cell biology perspective. Eur Respir J 55(4):2000607. https://doi.org/10.1183/13993003.00607-2020
118. Bigdelou B, Sepand MR, Najafikhoshnoo S et al (2022) COVID-19 and preexisting comorbidities: risks, synergies, and clinical outcomes. Front Immunol 13:890517. https://doi.org/10.3389/fimmu.2022.890517
119. Nicholson LB (2016) The immune system. Essays Biochem 60(3):275–301. https://doi.org/10.1042/EBC20160017

120. Zhang M, Wang P, Luo R et al (2021) Biomimetic human disease model of SARS-CoV-2-induced lung injury and immune responses on organ chip system. Adv Sci 8(3):2002928. https://doi.org/10.1002/advs.202002928
121. Si L, Bai H, Rodas M et al (2021) A human-airway-on-a-chip for the rapid identification of candidate antiviral therapeutics and prophylactics. Nat Biomed Eng 5(8):815–829. https://doi.org/10.1038/s41551-021-00718-9
122. Long C, Finch C, Esch M et al (2012) Design optimization of liquid-phase flow patterns for microfabricated lung on a chip. Ann Biomed Eng 40(6):1255–1267. https://doi.org/10.1007/s10439-012-0513-8
123. Sengupta A, Roldan N, Kiener M et al (2022) A new immortalized human alveolar epithelial cell model to study lung injury and toxicity on a breathing lung-on-chip system. Front Toxicol 4:840606. https://doi.org/10.3389/ftox.2022.840606
124. Konar D, Devarasetty M, Yildiz DV et al (2016) Lung-on-a-chip technologies for disease modeling and drug development. Biomed Eng Comput Biol 7(Suppl 1):17–27. https://doi.org/10.4137/BECB.S34252
125. Alberts B (2002) Molecular Biology of the Cell (4th Ed.). Garland Science, New York
126. Toepke MW, Beebe DJ (2006) PDMS absorption of small molecules and consequences in microfluidic applications. Lab Chip 6(12):1484–1486. https://doi.org/10.1039/b612140c
127. Campbell SB, Wu Q, Yazbeck J et al (2021) Beyond polydimethylsiloxane: alternative materials for fabrication of organ-on-a-chip devices and microphysiological systems. ACS Biomater Sci Eng 7(7):2880–2899. https://doi.org/10.1021/acsbiomaterials.0c00640
128. Zou W (2005) Immunosuppressive networks in the tumour environment and their therapeutic relevance. Nat Rev Cancer 5(4):263–274. https://doi.org/10.1038/nrc1586